

THE HOUSTON LIGHTNING MAPPING ARRAY: NETWORK  
INSTALLATION AND PRELIMINARY ANALYSIS

A Thesis

by

MATTHEW RYAN CULLEN

Submitted to the Office of Graduate Studies of  
Texas A&M University  
in partial fulfillment of the requirements for the degree of

MASTER OF SCIENCE

Chair of Committee,	Richard E. Orville
Committee Members,	Lawrence D. Carey
	Oliver W. Frauenfeld
Head of Department,	Ping Yang

August 2013

Major Subject: Atmospheric Sciences

Copyright 2013 Matthew Ryan Cullen

## ABSTRACT

The Houston Lightning Mapping Array (LMA) is a lightning detection network providing total lightning mapping for the Houston metropolitan area and southeast Texas. The network is comprised of twelve Very High Frequency (VHF) time-of-arrival total lightning mapping sensors built by New Mexico Institute of Mining and Technology and purchased by Texas A&M University. The sensors, installed in April 2012, are of the latest, modular design and built to be independent stations that utilize a solar panel for electricity and cellular data modems for communication. Each sensor detects the time of arrival of a VHF impulse emitted as part of the electrical breakdown and lightning propagation process. Data from each sensor are processed on a central LMA server to provide three-dimensional mapping of these impulses, also called LMA sources. This processing facilitates the analysis of variations in thunderstorm structure and the associated changes in both space and time.

The primary objectives for the installation of the Houston LMA network are twofold: first, to provide a dataset enabling research into thunderstorm electrification in the context of a coastal, urban, polluted environment; and second, to enable improvements in operational forecasting and public safety by providing total lightning data to partners including the National Weather Service (NWS). A workflow was established to create and share real-time data to these partners, while simultaneously maintaining a full, research-quality dataset. Data are retrieved from the field sensors and backed up to a central LMA server for processing and storage. Archived network data

are available from July 2012 through the present. The network measures 150 km from north to south, with stations in College Station and Galveston complementing the ten sites surrounding downtown Houston. This extends the region constrained by the network beyond the immediate metropolitan Houston area, resulting in increased accuracy in locating sources further from the network center. Based on initial analyses, the effective range of the Houston LMA is 75 km for three-dimensional mapping and approximately 250 km for two-dimension mapping.

## ACKNOWLEDGEMENTS

I would like to thank my advisor, Dr. Orville, for his guidance and support throughout this project. I would also like to thank Dr. Larry Carey and Dr. Oliver Frauenfeld for their service on my committee and dedication to review and provide feedback on my work. This project was supported by a grant from the National Science Foundation.

Additionally, I want to thank Mr. Dan Rodeheffer (New Mexico Tech) for his assistance deploying and installing the LMA sensors to the field and Dr. Eric Bruning (Texas Tech) for his instruction in LMA analysis techniques. Mr. Neil Smith and Mr. Richard Weitz greatly assisted with the installation and configuration of the local LMA processing server. This work would not have been possible without the contributions of these individuals.

To the faculty, staff, and fellow graduate students in the Department of Atmospheric Sciences, I extend my sincere appreciation for your contributions to my intellectual, professional, and personal growth.

I am thankful for my friends who have made Texas A&M not just a place of study, but also a home. You exemplify the notion of the Aggie Family and are the rock that has been my foundation of support throughout my time in College Station. Finally, to my parents, I am grateful for your unwavering support and encouragement that have made this entire journey possible.

## NOMENCLATURE

CG	Cloud-to-ground
IC	Intracloud
LDAR	Lightning Detection and Ranging
LMA	Lightning Mapping Array
NASA	National Aeronautics and Space Administration
NMIMT	New Mexico Institute of Mining and Technology
NWS	National Weather Service
TAMU	Texas A&M University
TOA	Time-of-arrival
VHF	Very High Frequency

# TABLE OF CONTENTS

	Page
ABSTRACT .....	ii
ACKNOWLEDGEMENTS .....	iv
NOMENCLATURE .....	v
TABLE OF CONTENTS .....	vi
LIST OF FIGURES.....	viii
1. INTRODUCTION.....	1
1.1 General Background and Motivation .....	1
1.2 Previous Studies .....	3
1.3 Research Objectives .....	5
2. DEVELOPMENT OF VHF LIGHTNING DETECTION TECHNIQUES.....	8
2.1 Early Development of VHF Lightning Detection Systems.....	8
2.2 Development of the Lightning Mapping Array .....	9
2.3 The National Lightning Detection Network.....	10
3. THE HOUSTON LIGHTNING MAPPING ARRAY .....	14
3.1 Basic Network Description .....	14
3.2 Typical Network Sensor Sites.....	21
3.3 Real-time Operation .....	25
3.4 Data Processing.....	28
4. DATA AND METHODOLOGY .....	30
4.1 Houston Lightning Mapping Array.....	30
4.2 National Lightning Detection Network.....	31
4.3 Network Range and Accuracy.....	31
4.4 Source and Flash Analysis .....	39
5. RESULTS.....	42

5.1 Network Location Accuracy .....	42
5.2 Network Range and Detection Capability .....	49
5.3 Operational Results .....	59
6. CONCLUSIONS .....	60
6.1 Conclusions .....	60
6.2 Future Work .....	61
REFERENCES .....	63

## LIST OF FIGURES

	Page
Figure 1. Map of current and planned Lightning Mapping Array installations around the United States. ....	11
Figure 2. Map of North American Lightning Detection Network (NALDN) sensor locations and effective network coverage.....	12
Figure 3. Schematic representation of the time-of-arrival (TOA) method to locate VHF sources in a three-dimensional lightning mapping network. ....	15
Figure 4. A five-panel plot depicting LMA sources grouped in a single flash over the Houston LMA network. ....	17
Figure 5. A plot showing the locations of the twelve sensors of the Houston Lightning Mapping Array, denoted by the green squares. ....	20
Figure 6. An image depicting a typical LMA site installation with the key external components labeled. ....	23
Figure 7. Image showing the inside of the LMA enclosure with key components labeled. ....	24
Figure 8. An image of the sensor site at Sugar Land Regional Airport depicting both the LMA (left) and LDAR-II (right) sensors. ....	26
Figure 9. Schematic representation of the geometry for locating the horizontal location of an LMA source within the network. ....	33
Figure 10. Schematic representation of the geometry for determining location uncertainty in the altitude of an LMA source within the network from the nearest LMA sensor. ....	35
Figure 11. Schematic representation of the basic geometry for locating an LMA source outside of the boundary of LMA sensors. ....	36
Figure 12. Screenshot of the xlma software package displaying ten minutes of Houston LMA data. ....	41
Figure 13. Plot of LMA sensors with primary baseline lengths overlaid. ....	44



Figure 14. Plot of calculated reduced chi-square compared to theoretical chi-square distribution for 25ns timing error for the thirty minute period from 23:00 to 23:30 UTC on May 6, 2012. ....	46
Figure 15. Five panel plot of VHF sources from the Houston LMA from 23:00 to 23:30 UTC on May 6, 2012. ....	47
Figure 16. Plot of fraction of total sources detected by each sensor for the thirty minute period from 23:00 to 23:30 UTC on May 6, 2012. ....	48
Figure 17. Schematic illustration the heights of blockage of VHF sources by a 1-degree elevation angle obstruction at a sensor site. ....	50
Figure 18. One hour plot of LMA sources detected from 09:00 to 10:00 UTC on May 12, 2012 illustrating the impact of the curvature of the earth when detecting sources at a distance from the network center. ....	51
Figure 19. Radar reflectivity from KHGX radar at 15:59 UTC on May 10, 2013 showing the line of strong storms pushing southeast through the Houston metropolitan area. ....	53
Figure 20. Plot of CG strikes from the NLDN from 15:45 to 16:15 UTC on May 10, 2013. ....	54
Figure 21. LMA point sources from 15:45 to 16:15 UTC on May 10, 2013. ....	56
Figure 22. Same as Figure 21 but for LMA source density. ....	57
Figure 23. LMA sources and NLDN ground strikes detected from 23:30 to 23:40 UTC on May 6, 2012. ....	58

# 1. INTRODUCTION

## **1.1 General Background and Motivation**

Recent research in the atmospheric sciences has shifted to seeking to understanding severe weather events with significant ability to impact the lives of individuals, in terms of property damage and personal injury or death. While it does not instantly impact large numbers of individuals as seen with hurricanes, tornadoes, and flooding, lightning is responsible for a large number of casualties throughout all months of the year. As noted by Curran et al. (2000), only floods killed more people per year in the United States from 1959 to 1991. In the most recent 30-year average available from the National Weather Service, covering the period from 1982 through 2011, lightning is still a major component of weather-related fatalities passed only by flooding and tornadoes. While the particularly deadly 2011 tornado season coupled with recent public information campaigns featuring lightning safety guidelines dropped lightning to the third most fatal type of weather event, more than 50 people per year are killed by lightning. Furthermore, lightning is responsible for lost productivity in many important industries, most notably aviation. Thus, there is significant value in mapping electrical structure to improve our understanding of electrification patterns and processes within thunderstorms.

The Houston Lightning Mapping Array (LMA) is a three-dimensional total lightning mapping system encompassing the Houston, Texas metropolitan area and southeast Texas. The Houston LMA was installed in mid-April 2012 and is comprised of

twelve very high frequency (VHF), time of arrival (TOA), total lightning mapping sensors built by New Mexico Institute of Mining and Technology and purchased and operated by Texas A&M University. Each sensor detects the time of arrival of a VHF impulse emitted as part of the electrical breakdown and lightning propagation process. The mapping of these impulses, also called sources, facilitates the analysis of variations in thunderstorm structure and the associated changes in both space and time. The primary objectives of the Houston LMA are twofold: first, to provide a dataset enabling research into thunderstorm electrification in the context of a coastal, urban, polluted environment; and second, to enable improvements in operational forecasting and public safety by providing total lightning data to the Houston/Galveston Forecast Office of the National Weather Service (NWS).

The establishment of a total lightning mapping system for Houston, Texas is particularly useful for the study of various weather phenomena as the region is climatologically susceptible to thunderstorm activity year-round. Additionally, cold fronts, sea breeze influences, mesoscale convective systems, and even tropical cyclones impact southeast Texas and provide a unique diversity of future cases for study of electrification development and structure. Houston is one of the most polluted cities in the United States, and this network will enable further investigation into the impacts of increased aerosol loading on the development and structure of electrification processes. Finally, the Houston metropolitan area is the fourth most populous in the United States, and access to the Houston LMA data serves as a decision support tool to assist the NWS in its mission to protect life and property. Therefore, the installation of the Houston

LMA network, particularly in conjunction with data from the National Lightning Detection Network (NLDN), enables us to address outstanding questions about cloud-to-ground (CG) and intracloud (IC) flashes that together characterize the total lightning over Houston, Texas and the surrounding area. This combination of LMA and NLDN data enable analysis of flashes to determine many parameters including location, polarity, and peak current of the ground flash, total flash rate, CG flash rate, IC/CG ratio and information related to the initiation point and flash extent of both CG and IC flashes.

## **1.2 Previous Studies**

Following the development of the Lightning Mapping Array system in the mid-1990s at New Mexico Institute of Mining and Technology, Rison et al. (1999) and Krehbiel et al. (2000) published initial work detailing the operation and mapping of the total lightning sources in central New Mexico and Oklahoma, respectively. The North Alabama LMA, maintained by NASA's Marshall Space Flight Center, has been continuously operating since 2002 and has provided insight into tracking lightning jumps, or sudden increases in total lightning flash rates. After these initial studies yielded positive results, the LMA was a central instrument in the Severe Thunderstorm Electrification and Precipitation Study (STEPS) field campaign during summer 2000 based in eastern Colorado and northwestern Kansas. STEPS provided an opportunity to verify location and polarity of the lightning channel mapped by the LMA via in situ aircraft observations and sounding balloon observations (Warner et al., 2003; Thomas et al., 2004). While electrification studies were only a component of research and data collection in STEPS, they were a primary goal in the Thunderstorm Electrification and

Lightning Experiment (TELEX) held in Oklahoma in the summer of 2003 and 2004. In this field campaign, a primary goal of the work was collecting comprehensive datasets to further study inverted-polarity storms and stratiform regions of mesoscale convective systems (MCSs) while also developing practical operational uses of lightning data (MacGorman et al., 2008). Using the data collected during the TELEX project, progress has been made to advance understanding and knowledge in the areas of these goals. Investigations into total lightning structure within mesoscale convective systems over Houston were conducted by Ely et al. (2008) following the installation of the Houston LDAR-II network.

The impact of the aerosol effect upon cloud electrification can be investigated through the data collected by the Houston LMA. Previous studies have established that urban heat island effects and anthropogenic aerosol effects influence both lower tropospheric chemistry and cloud electrification (Rosenfeld and Lensky, 1998). Earlier work has established interconnected relationships between convective development, rainfall, and lightning (Huff and Changnon, 1973; Westcott, 1995; Shepherd et al, 2002). Anthropogenic influences have been hypothesized as a potential explanation for positive rainfall and lightning anomalies discovered over and downwind of the Houston metropolitan area (Orville et al., 2001; Steiger et al., 2002; Shepherd and Burian, 2003). As noted by Westcott (1995) and Shepherd et al. (2002), these urban signals in CG lightning and rainfall have additionally been noted over and downstream of other major cities in the United States.

Several studies have been completed using data collected during the previously mentioned STEPS and TELEX field campaigns. Individual flashes can be manually visualized and analyzed through the inferred charge identification technique. As noted by Tessendorf et al. (2007), numerous studies including MacGorman et al. (2005) and Wiens et al. (2005) have investigated predominately positive CG storms from these datasets, while that study focused on storms lacking positive CGs. Therefore, the development of case studies featuring diverse electrification characteristics can be useful to gain insight into the mechanisms behind such differences. MacGorman et al. (2011) performed analyses of the timing total lightning data in relation to occurrence of CG lightning in three different regions; namely, north Texas, Oklahoma, and the high plains of Colorado, Kansas, and Nebraska. This study noted that storms on the high plains exhibited longer times between start of lightning activity and the first CG than thunderstorms in Oklahoma and north Texas, which is consistent with previous work showing that CGs make up a lesser percentage of total lightning in the high plains region than in the rest of the contiguous United States.

### **1.3 Research Objectives**

Following the installation of the network and the establishment of a data workflow and system of processing, the actual analysis of data from the Houston LMA network can begin. As such, there are numerous research goals to this work which are best grouped under two comprehensive objectives: 1) to detail the instrumentation, typical site setup, installation, operation, and dissemination of data from the Houston

LMA and 2) to characterize total (CG and IC) lightning activity using the Houston LMA in conjunction with data from the National Lightning Detection Network (NLDN).

The first objective involves describing the installation of the network and subsequent process to establish the workflow for processing Houston LMA data. During one week in mid-April 2012, eleven stations were built and deployed to the field. The components of the sensor, the configuration of the sensor site, and the means of recording, storing, and transmitting data for processing will be discussed. Each station in the network is configured to decimate and transmit data in a real-time processing mode, while also simultaneously writing the full raw data to an internal storage hard drive. The real-time data are processed on a central server and used to generate a publically accessible webpage displaying both 2-minute and 10-minute images of LMA sources and LMA source density. The real-time data are also distributed to partners including the National Weather Service for use in forecasting applications and development of new products. The raw data are sent to a central server once a day where it can be post-processed for analysis. The establishment of a processing workflow and archival plan will facilitate the incorporation of the Houston LMA data in future studies.

The second objective will involve the initial analysis of the storms detected by the Houston LMA network. We will first evaluate the effective range of the Houston LMA network by considering limitations of network operations. Then, we will establish a recommendation for future studies utilizing this dataset by investigating the number of sources detected by the LMA network as a function of distance and direction from the network center. Multiple storm events will be investigated to determine the

characteristics of the Houston LMA network's detection accuracy and efficiency. After grouping detected LMA sources into flashes using an algorithm developed at New Mexico Institute of Mining and Technology, we will then utilize the inferred charge identification technique to analyze flashes within storms. In addition to the identification and classification of the charge regions, the LMA data will be compared to data from the NLDN to evaluate the timing and detection of CG lightning versus total lightning within a storm.



## 2. DEVELOPMENT OF VHF LIGHTNING DETECTION TECHNIQUES

### 2.1 Early Development of VHF Lightning Detection Systems

In his field experiments in South Africa, D. E. Proctor was among the first to utilize VHF sources to investigate electrification within thunderstorms (Proctor, 1971). Proctor established a five-sensor network placed along perpendicular baselines, with the analog data signal transmitting from each of the 4 outer sensors back to a data recorder located with the middle station. He utilized the time of arrival (TOA) method to examine the electrical breakdown of an individual flash of lightning. By determining the difference in time of arrival, the location of the source can be calculated by a series of hyperbolic formula. In this system, root mean square location error was about 25 meters in the horizontal directions. However, horizontal location errors were significantly larger, ranging from 100 meters to over 1 kilometer depending both on the height of the source and on the distance of the source from the network center.

Utilizing the same TOA principles, Lennon developed the Lightning Detection and Ranging (LDAR) network in the mid-1970s. This network enabled the mapping of lightning activity above the Kennedy Space Center (KSC), located in Florida. This seven-sensor system was arranged in a circular pattern with a station in the middle. Like Proctor's earlier system, the LDAR network transmitted analog data. However, LDAR digitized the received data at 50 ns resolution over 100 microsecond intervals that enabled automatic, real-time processing (Poehler and Lennon, 1979). This enabled the system to map several tens of sources per flash, as noted by Lhermitte and Krehbiel

(1979). While this number is meager in today's terms, the ability to process in real time was a significant advance in VHF lightning detection technology. Lennon and colleagues upgraded the KSC LDAR network to a second-generation system in the early 1990s, which increased detection effectiveness and enabled processing of up to 10,000 sources per second (Maier et al., 1995; Ely et al., 2008).

## **2.2 Development of the Lightning Mapping Array**

Developed by the New Mexico Institute of Mining and Technology (hereafter, New Mexico Tech), the Lightning Mapping Array (LMA) represented a significant breakthrough in VHF lightning mapping technology. The LMA was developed in the mid-1990s at New Mexico Tech and was first installed in a research setting in central Oklahoma in 1998 (Krehbiel et al., 2000). As noted by Rison et al. (1999), the functional operation of an LMA instrument is based upon the previously discussed LDAR system at NASA's KSC in Florida. However, the inclusion of a Global Positioning System (GPS) receiver at each sensor enables the time of arrival to be independently measured at each LMA station site. Furthermore, each source is recorded and digitized at the sensor, enabling storage on a hard drive locally. Thus, each LMA station could operate autonomously, in contrast to the LDAR sensors that required all data to be directed to a central station. The LMA time of arrival source observations could then be transmitted via either wireless communication links or the Internet to a central location for real-time processing, enabling both research and operational analysis applications (Krehbiel et al., 2000; Rison et al., 1999). This enabled the sensor to operate independently and continuously without manual operator action to produce three-dimensional mapping and

timing of lightning flashes. After the initial deployment in Oklahoma in June 1998, the LMA was tested near Langmuir Laboratory in Socorro, New Mexico in August and September of the same year (Rison et al., 1999) The LMA became a key element of a field campaign, the Severe Thunderstorm Electrification and Precipitation Study (STEPS), which occurred during summer 2000 in northwestern Kansas and eastern Colorado. This field project collected flight track and sounding balloon observations that resulted in a thorough evaluation of LMA network accuracy by Thomas et al. (2004). The first continuous operational LMA started in late 2001 with the installation of the North Alabama LMA, centered over Huntsville, Alabama (Goodman et al, 2005). Subsequent networks were installed with the goal of real-time operation and development of research applications in Oklahoma and in New Mexico at White Sands Missile Range (Thomas et al., 2004). More recently, additional networks were established in Washington, D.C., west Texas, and Colorado, the latter as part of the Deep Convective Clouds and Chemistry (DC3) field campaign. A map of current LMA networks is shown in Figure 1.

### **2.3 The National Lightning Detection Network**

Detection of CG lightning discharges began in the late 1970s following the invention of a magnetic detection finder combined into an automated signal processor (Krider et. al. 1980). These instruments were deployed in the western United States and Alaska by the Bureau of Land Management to assist in applications of wildland fire mitigation. In the ensuing years, other regional networks began to take shape around the United States. A network deployed in Oklahoma was unique in its prime location to

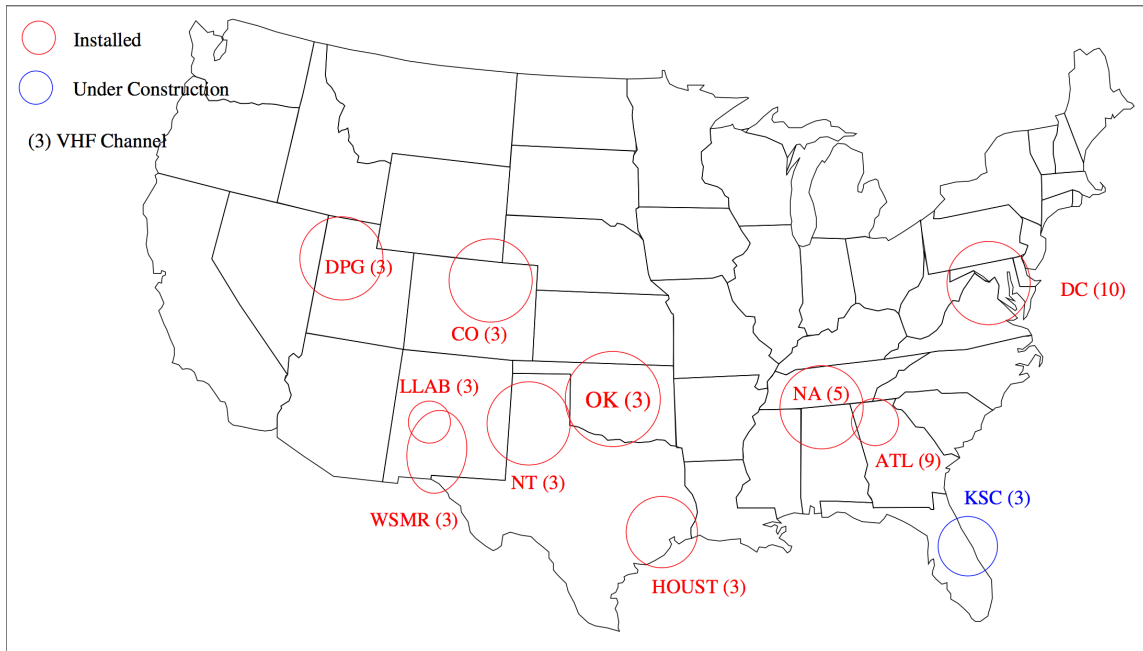


**Figure 1.** Map of current and planned Lightning Mapping Array installations around the United States. An LMA network has also been installed in eastern France and another is planned for installation later this year in Corsica.

observe severe thunderstorm and tornado outbreaks. An operations control center was established in spring 1982 at the State University of New York at Albany for a network in the northeastern United States, and within a year, this network contained ten sensors providing coverage extending to North Carolina. By the end of 1988, these regional networks expanded and combined to provide complete coverage of CG lightning for the contiguous United States (Orville 2008). The network operation transitioned from academia to commercial operation in the early 1990s, and today Vaisala, Inc. maintains operation and maintenance responsibility out of its NLDN Network Control Center in

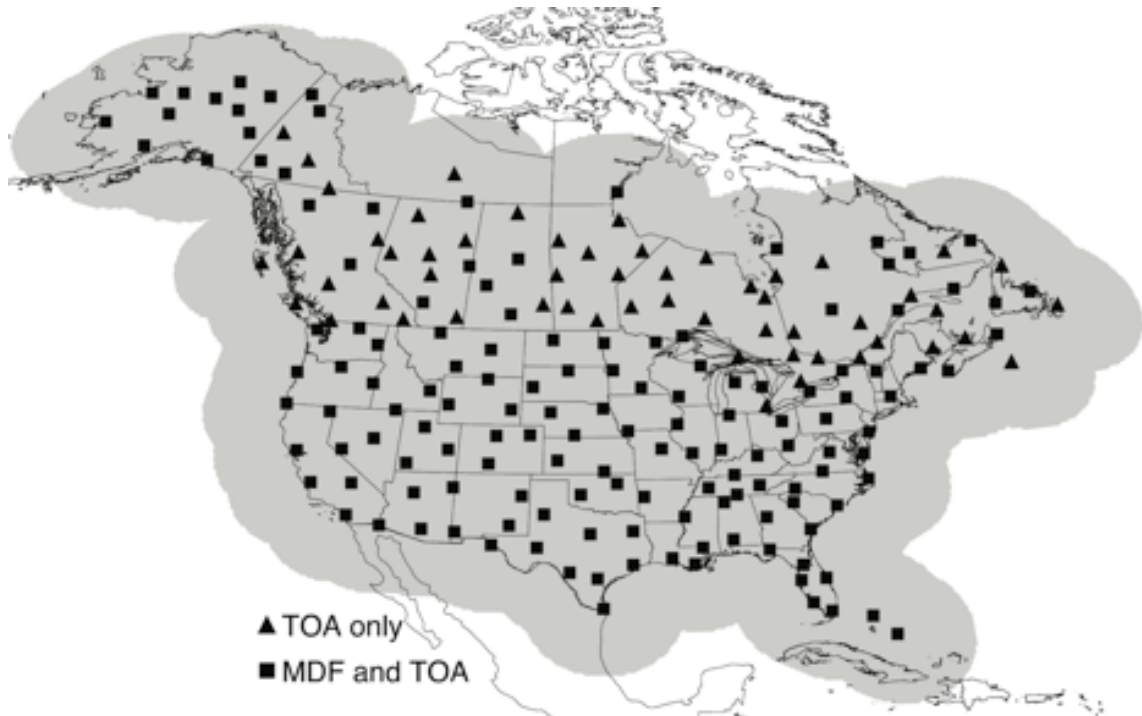


**Figure 2.** Map of North American Lightning Detection Network (NALDN) sensor locations and effective network coverage. Note that the NALDN is simply the combination of both the NLDN and the Canadian Lightning Detection Network (CLDN).

Tucson, Arizona. The system has undergone three significant upgrades, one in the mid 1990s, another in the early 2000s, and the most recent in 2012, which have increased the sensitivity and number of sensors within the network. More than 100 sensors comprise the current network, and a map of their locations and effective range is displayed in Figure 2. The NLDN detects more than 95% of CG flashes with a median location accuracy of 250 meters or better over the contiguous United States. Archived data from

this network are received at Texas A&M monthly on compact disc, and the specifics of this will be detailed in the data and methodology section of this thesis.

### 3. THE HOUSTON LIGHTNING MAPPING ARRAY

#### **3.1 Basic Network Description**

Mapping of total lightning in the Houston, Texas metropolitan area began in summer 2005 when a network of LDAR-II sensors was established with the purpose of conducting detailed research into the enhancement of electrification within the context of a major urban city center (Orville et al., 2001). Ten sensors installed in July 2005 formed the initial network, with the transmission of the data to the central processing server on the campus of Texas A&M commencing in August of the same year. Two additional sensors were added to the network in January 2007, bringing the Houston LDAR-II network to a full set of twelve stations. These sensors were purchased from Vaisala, Inc. who developed a commercial version of the original Kennedy Space Center LDAR sensors following improvements that came about due to collaboration with researchers at New Mexico Institute of Mining and Technology (Thomas et al., 2004). As noted by Ely et al. (2008), the LDAR-II sensors were functionally similar to the Lightning Mapping Array sensors developed at New Mexico Institute of Mining and Technology. The Houston LDAR-II network remained operational until March 2012 when the network was decommissioned and subsequently replaced by the Houston Lightning Mapping Array (LMA). The Houston Lightning Mapping Array network is a system of twelve total lightning VHF detection sensors installed around the greater Houston metropolitan area and southeast Texas. This network of sensors was purchased by Texas A&M University from New Mexico Institute of Mining and Technology in Socorro, New

Mexico to facilitate three-dimensional mapping of electrical activity over a coastal, large metropolitan city. This mapping serves two key purposes: 1) to provide a dataset for detailed studies of the impact of the urban environment on the structure of thunderstorm development and 2) to provide real-time lightning data to forecasters at the Houston/Galveston National Weather Service Forecast Office. This LMA network replaces the Houston Lightning Detection and Ranging (LDAR-II) network that was in place from July 2005 until March 2012. As noted above, the LDAR-II and LMA sensors are functionally similar, though the LMA sensors installed in Houston have undergone iterative enhancements to increase portability and reduce power consumption.

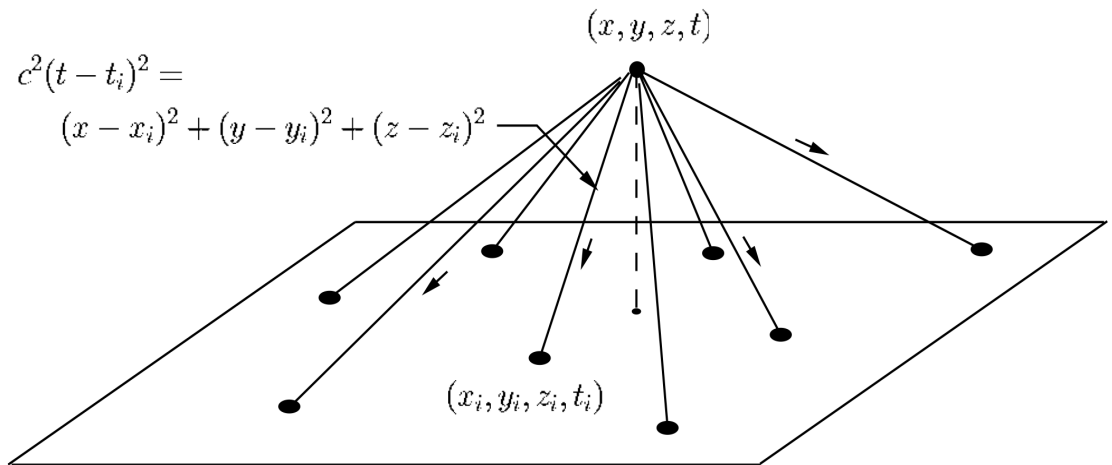


**Figure 3.** Schematic representation of the time-of-arrival (TOA) method to locate VHF sources in a three-dimensional lightning mapping network. The time and position of the arrival of the source at each sensor for at least 4 sensors can be used to solve a system of equations to locate the time and position  $(x, y, z, t)$  of the VHF point source. (Thomas et al., 2004)



A total lightning mapping system detects the impulses of radiation that are emitted during the breakdown and channel propagation processes in electrified storms. As with all other LMA networks, the Houston LMA system utilizes a Global Positioning System (GPS) equipped receiver in the VHF frequency space to detect the time of arrival of these LMA sources (Rison, 1999). Each station individually records the time of arrival and the peak power received for a source and transmits this information to a central server for processing (Thomas et al., 2001). Using the time of arrival technique, the precise time a source is detected at each of multiple stations enables the solving of a system of equations revealing the time and location of origin of the VHF source, as schematically illustrated in Figure 3 (Thomas et al., 2004). After undergoing processing, the resulting solutions reveal the time and location of the LMA sources. These LMA sources can further be grouped into flashes using spatial and temporal criteria and subsequently displayed on a plot, as in Figure 4.

The Houston LMA became operational during the week of April 15, 2012 when the first eleven sensors of the network were installed in the field. Data from these stations were initially transmitted to a central server located at New Mexico Institute of Mining Technology. Real-time processing commenced in late April and data became publicly available on the Internet on April 29, 2012. The Houston LMA operated with eleven sensors until the network installation was completed with the deployment of the twelfth sensor to the campus of Texas A&M University – Galveston on Pelican Island on August 22, 2012.

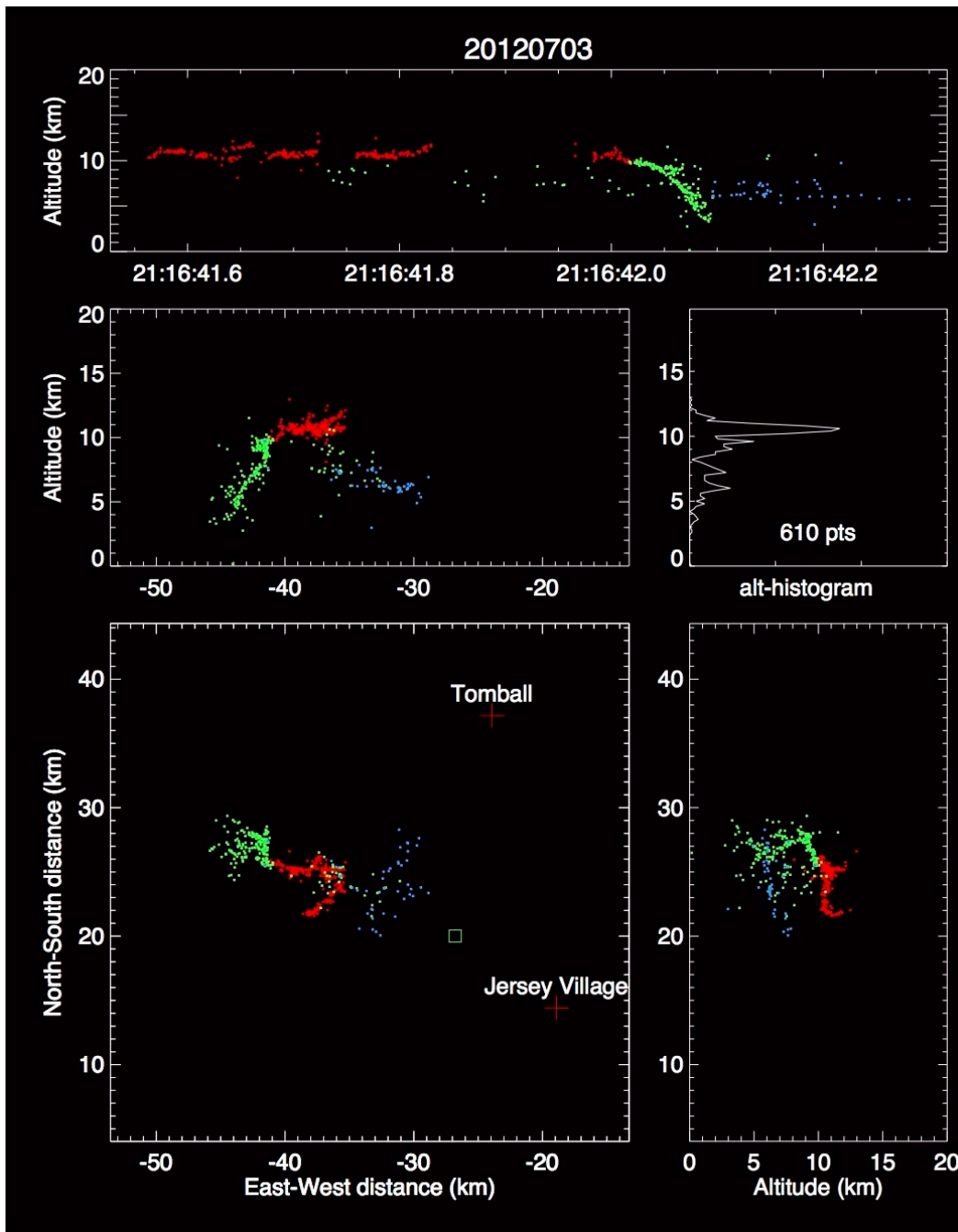


**Figure 4.** A five-panel plot depicting LMA sources grouped in a single flash over the Houston LMA network. The points are colored red (blue) to denote their inferred positive (negative) charge. From top-to-bottom, left-to-right, the panels plot 1) time vs. height, 2) east-west distance vs. altitude, 3) a histogram of points by altitude, 4) east-west distance vs. north-south distance (plan view), and 5) altitude vs. north-south distance.

The Houston network is centered just northwest of the Houston central business district at 29.76 N, 95.37 W. The core of the network is comprised of ten sensors that surround the greater Houston area with a radius of approximately 35 kilometers. Each station is spaced about 25 kilometers from the adjacent sites, though this distance is slightly larger on the east side of the network. Each of these ten locations was previously utilized as a location in the previous LDAR-II network. The two remaining LDAR-II sites were not utilized for the new LMA network due to a combination of access limitations and proximity to sources of relatively high RF noise. Instead, the two final sensors were located in Galveston and College Station. The Texas A&M University – Galveston site is located approximately 70 kilometers from the network center, while the sensor in College Station is about 130 kilometers from the midpoint of the network. The locations of the twelve sensor sites are mapped in Figure 5 and presented in tabular form in Table 1.

Each sensor is tuned to detect the time of arrival of a VHF pulse by listening in the 60 to 66 MHz range, the space associated with analog television channel 3. The previous LDAR-II network operated optimally in this range, so this LMA network was configured to use the same frequency to eliminate the need for additional site noise surveys prior to network installation. In order to maximize the accuracy of VHF source locations, the optimal spacing is to situate a sensor with 20-30 kilometer spacing between adjacent network sensors (Ely et al., 2008). However, as was required with the LDAR-II installation, some compromises were required due to the distribution of acceptable sites and proximity of potential sites to sources of noise such as power lines.

**Table 1.** Locations of the sensors in the Houston Lightning Mapping Array.

Number	Sensor ID	Location	Latitude	Longitude
1	A	Cy-Fair ISD Cypress, TX	29.939° N	95.646° W
2	B	Williams Airport Porter, TX	30.157° N	95.320° W
3	C	Johnson Space Center Houston, TX	29.567° N	95.098° W
4	D	Sugar Land Regional Airport Sugar Land, TX	29.619° N	95.658° W
5	F	Houston Southwest Airport Arcola, TX	29.505° N	95.476° W
6	G	Addicks Reservoir Houston, TX	29.768° N	95.645° W
7	H	Royal Purple Raceway Baytown, TX	29.791° N	94.883° W
8	I	Texas A&M University College Station, TX	30.646° N	96.298° W
9	J	Lone Star College – North Harris Houston, TX	30.002° N	95.384° W
10	K	Alvin ISD Alvin, TX	29.441° N	95.273° W
11	L	May Community Center Huffman, TX	30.058° N	95.061° W
12	M	Texas A&M – Galveston Galveston, TX	29.316° N	94.822° W

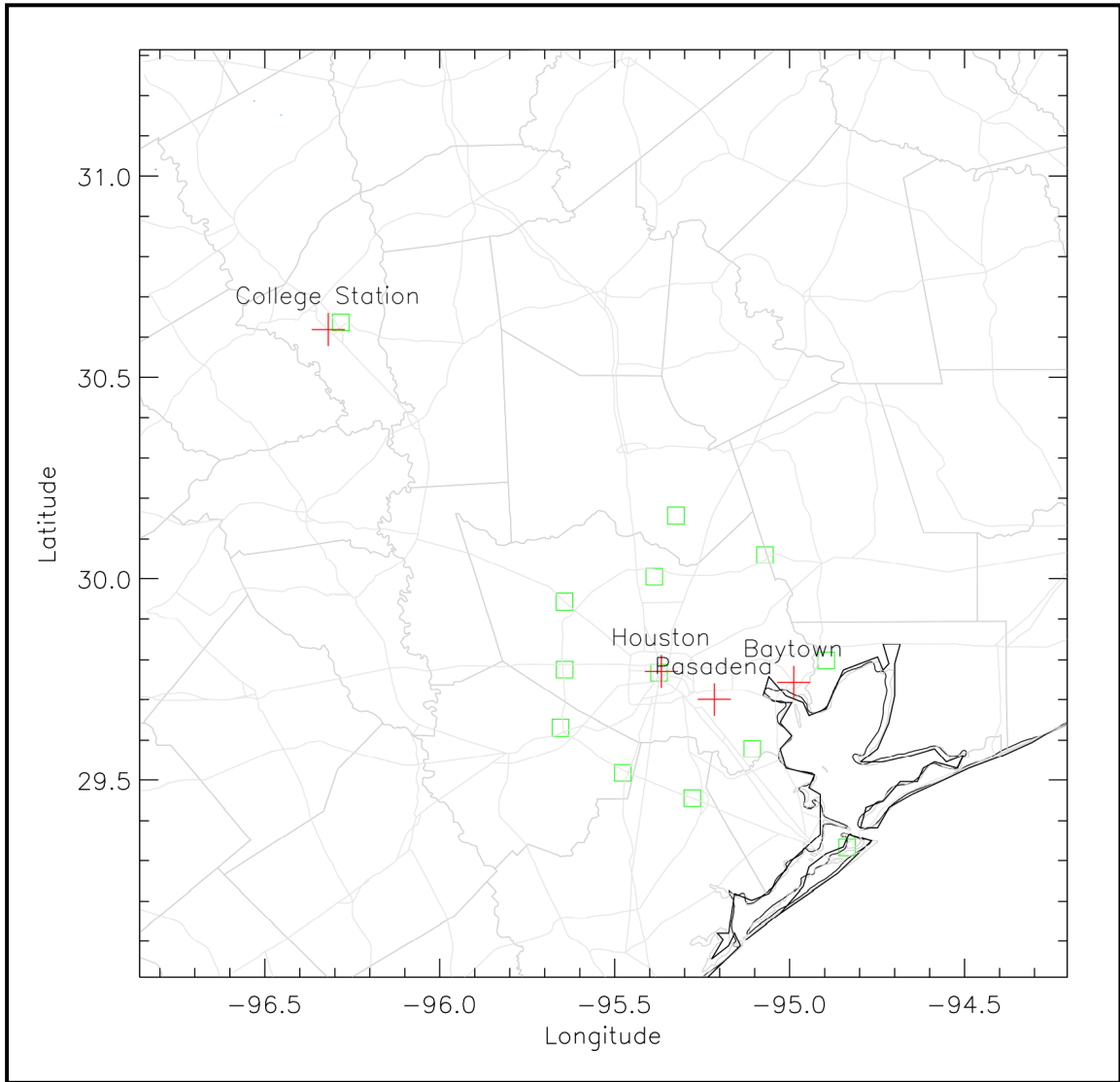


**Figure 5.** A plot showing the locations of the twelve sensors of the Houston Lightning Mapping Array, denoted by the green squares. Ten sensors surround downtown Houston, while the eleventh and twelfth are located in College Station and Galveston, respectively.

The addition of the Galveston and College Station sensor sites enhances the range of the network towards the southeast along the Texas coastline and northwest of the network center, respectively. Additionally, locating a site in College Station places a site in close proximity to the Texas A&M campus for convenient access when troubleshooting and performing network maintenance.

### **3.2 Typical Network Sensor Sites**

As noted previously, ten of the sensor site locations from the LDAR-II network were utilized for the installation of the new LMA sensors. These stations form the core of the Houston network and surround the Houston metropolitan area. The remaining two sites, both located within the outer ring of stations, were not used for both logistical and technological reasons. Due to the line-of-sight nature of propagation of emitted VHF sources, locations selected should have a clear view of the sky. Following the general guidelines utilized for the installation of the LDAR-II, no more than 1 degree above the horizon should be blocked by nearby obstructions (Ely, 2008). As a result, the two sites near the center of the Houston area had the LDAR-II stations installed on the roof of local buildings to avoid blockage of signal from large buildings. Access to these sites required non-trivial ladder climbs (approximately 25 feet), which complicates the movement of supplies for maintenance trips, and cranes would have been necessary to move portions of the sensor installation to the roof. Therefore, alternative sites were selected to simplify logistical needs both at the time of installation and in the future. Ultimately, the sensors at all of the LMA sites are situated in areas of relatively low ambient noise, no immediate proximity to power lines, radio towers, or flood lights

(which are capable of causing temporary high RF noise), and locations with minimal to no obstructions to the horizon.

The standard LMA sensor utilized for the Houston LMA network is designed and manufactured at New Mexico Institute of Mining and Technology and is the latest iteration of the portable LMA sensor design. The general station consists of a roughly 4'x3'x2' construction site job box attached to a frame built with plated steel. Two poles are mounted on the steel frame, one on each side, to attach the VHF antenna and cellular modem antenna, while the GPS antenna is attached on the side of the steel frame. A solar panel is attached across the front of the frame to provide power for the entire system and additionally serves to shade the job box. These external components are identified in Figure 6. The job box contains the LMA enclosure and two deep cycle marine batteries to power the system. The LMA enclosure, detailed in Figure 7, is a sealed box containing the key electronics for the sensor, including the receiver, processor, GPS, cellular data modem, and a hard drive disk for onsite storage.

In order to increase flexibility in site installation to situate the sensor in the lowest RF noise area at a particular site, the sensor is built to be independent and self-sufficient in that wired power or Internet connections are not required. A 135 W solar panel provides charge to two deep cycle marine batteries stored within the construction job box. These batteries are capable of powering the system for about three days from full charge without additional solar charging, enabling continued operation of the sensor during periods of cloudy skies. The sensor design also eliminates the need for wired ethernet lines or a wireless bridge. The entire Houston metropolitan area and

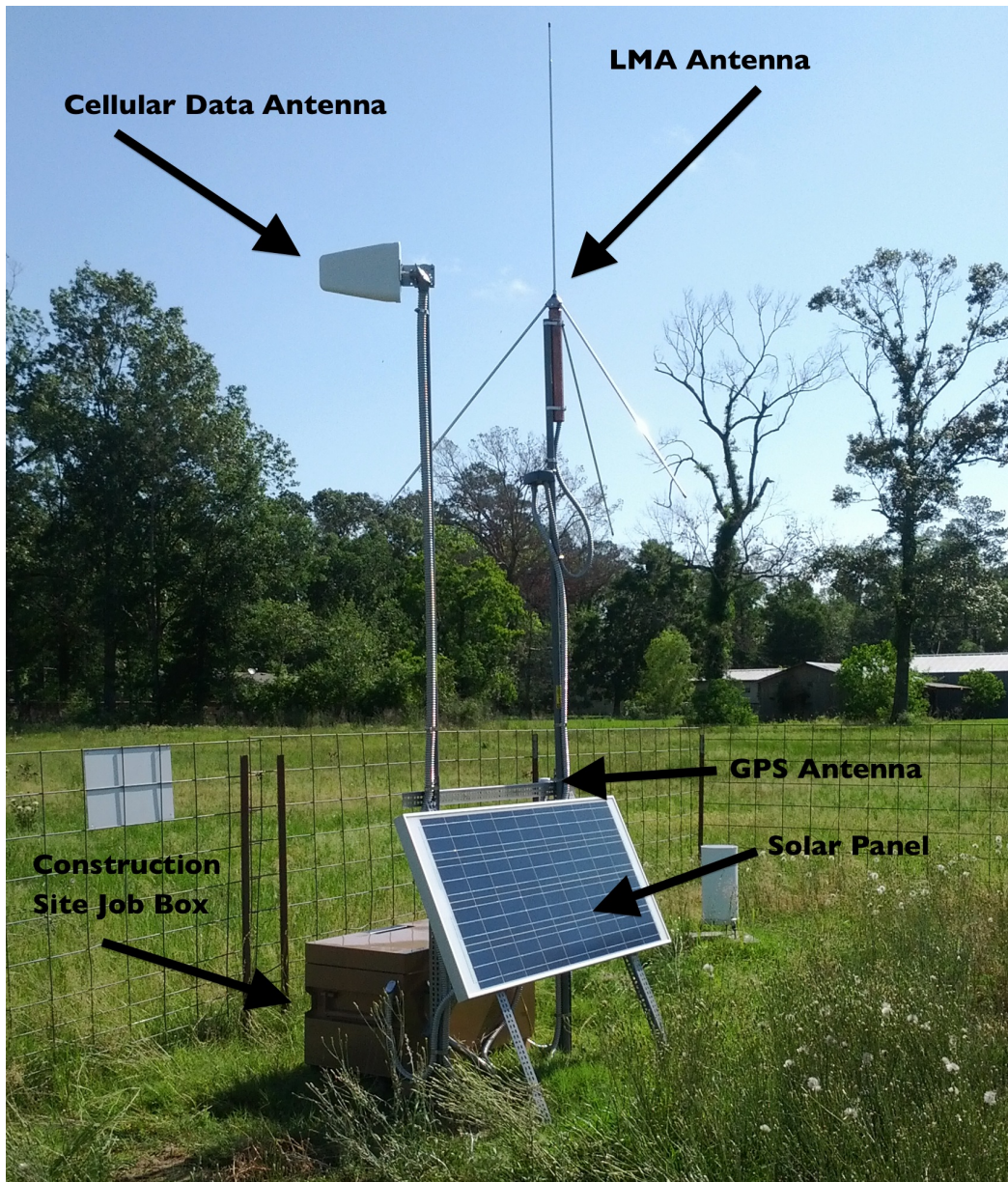


**Figure 6.** An image depicting a typical LMA site installation with the key external components labeled. This photo shows the sensor located at Williams Airport in Porter, TX. The construction site job box contains two deep-cycle marine batteries and the LMA enclosure.



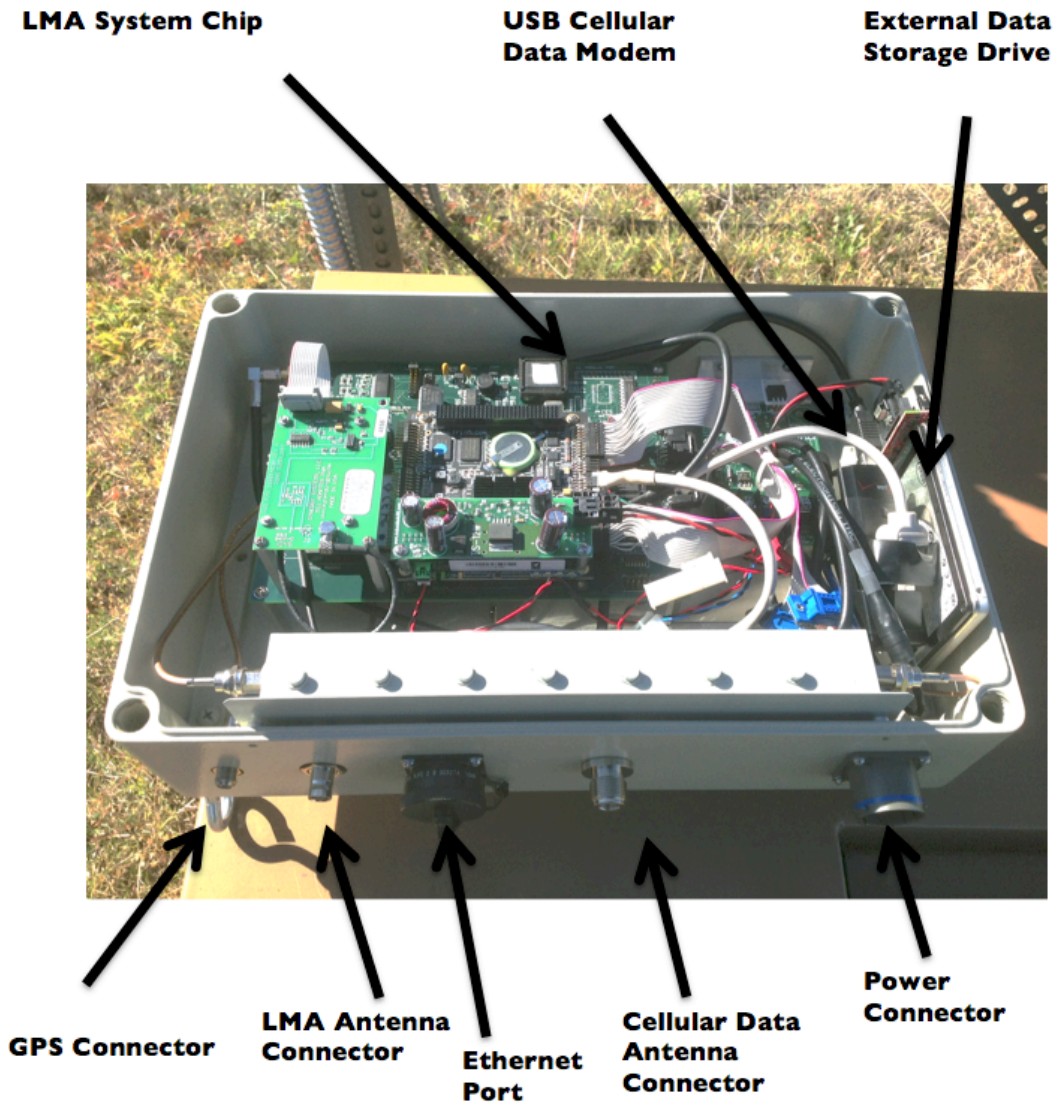


**Figure 7.** Image showing the inside of the LMA enclosure with key components labeled.

surroundings are well covered by the major cellular carriers. We utilize a USB cellular data modem installed within the LMA enclosure to maintain communications with a central LMA processing server. In the event that the cellular connection is lost or unavailable for a period of time, the external hard drive disk is available to store data until the network connection is restored. The steel frame is secured by the weight of the construction site job box and batteries and reinforced by four stakes that anchor the frame. The enhanced independent nature and more portable design of the LMA stations mark a significant improvement over the LDAR-II sensors that featured large (30 feet tall) mast antennas and were mounted on cement pedestals. The differences in footprint is clearly evident, as shown in Figure 8, which depicts the LMA and LDAR-II sensors side-by-side at the Sugar Land Regional Airport sensor site.

### **3.3 Real-time Operation**

The Houston LMA system is configured to enable real-time processing of the LMA source time and location solutions. This enables forecasters, researchers, and other interested individuals to view the locations of VHF sources in real-time. As previously mentioned, the Houston LMA network utilizes cellular data modems to facilitate communication from the field sensors. This enables stations to be situated far from buildings without the need for external wireless antennae or buried ethernet line back to an Internet source. Furthermore, this prevents changes to the host site's Internet configuration from blocking or limiting access to a sensor.

This communication link enables the sensor to communicate to a central operations server where operation of the network can be monitored and real-time

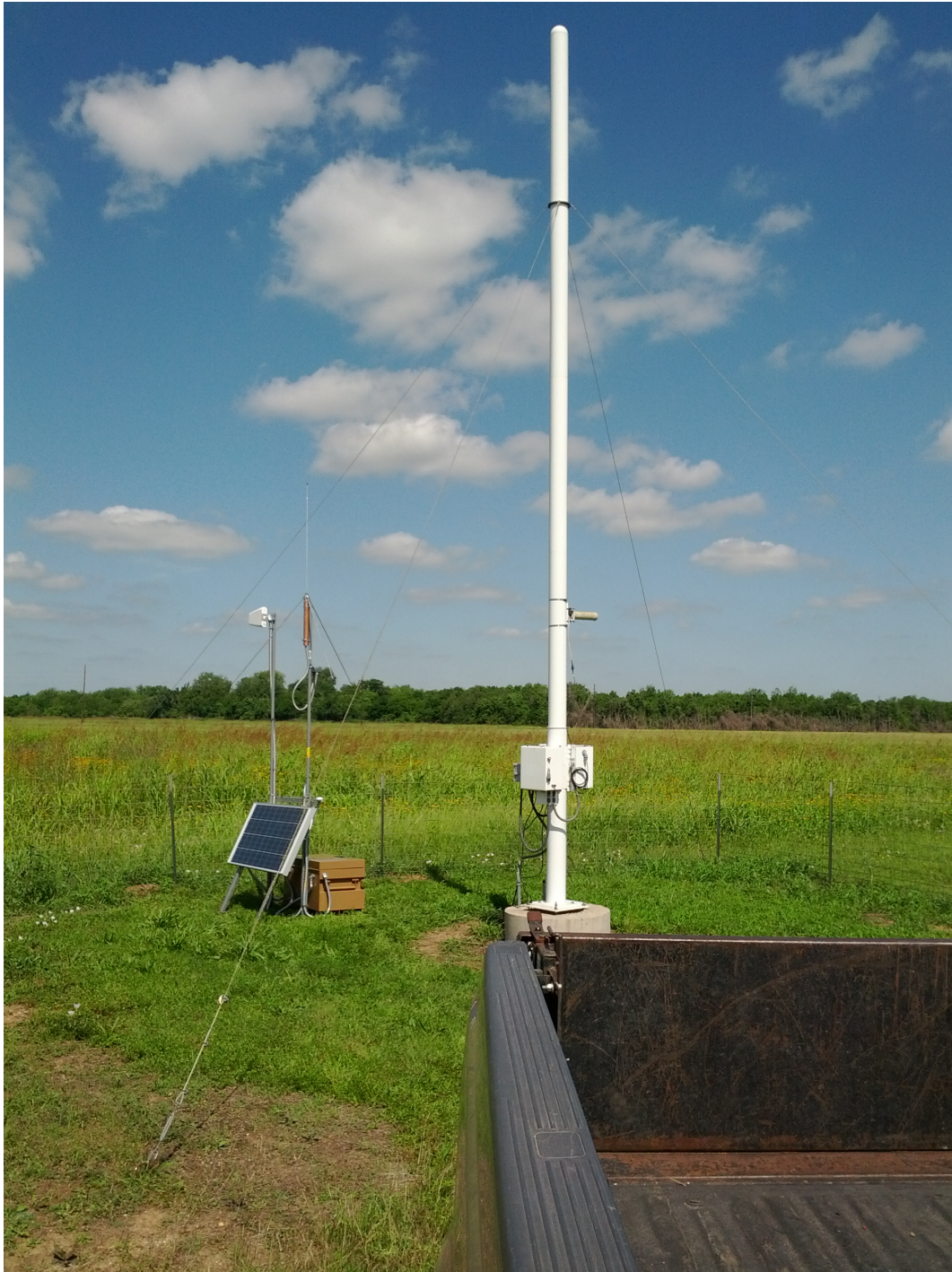


**Figure 8.** An image of the sensor site at Sugar Land Regional Airport depicting both the LMA (left) and LDAR-II (right) sensors. Note that the LDAR-II sensor contains a much larger mast and is installed on a cement pedestal, while the LMA sensor utilizes a more compact design.

processing, display, and analysis of the data can occur. The LMA processing chip, in conjunction with the GPS device, determines and records the precise moment the VHF source is received by the LMA antenna. The LMA can detect a pulse from a source every 80 microseconds, known as one window, which corresponds to a maximum detection rate of 12,500 sources per second. These files are stored to the local data disk, but a decimation process is used to facilitate real-time processing given bandwidth constraints. The system records the largest event among five consecutive windows, or 400 microseconds, and sends the time, peak amplitude, and other diagnostic information in real-time to a central processing server.

Data from each of the sensor sites are received and processed by a central LMA server and pushed to a Local Data Manager (LDM) server for real-time distribution. This enables partners, such as the National Severe Storms Laboratory (NSSL) in Norman, Oklahoma, NASA's Short-term Prediction Research and Transition Center (SPoRT) in Huntsville, Alabama, the Spaceflight Meteorology Group (SMG) at Johnson Space Center, and local National Weather Service Weather Forecasting Offices (NWS WFOs), to ingest this data as part of their operational forecasting workflow. This facilitates the use of Houston LMA data in various operational and research applications, including the Hazardous Weather Testbed (HWT) Spring Experiment, the National Lightning Jump Field test, and GOES-R Proving Ground activities. WFO Houston/Galveston has noted value in utilizing Houston LMA data in the operational setting, and this will be discussed in a later section. Additionally, 2-minute and 10-minute plots of both point sources and source density are generated and updated each minute. Each of these plots displays a 3-

panel chart with data visualized in x-y (plan view), x-z, and y-z space. These real-time images are available on the Houston LMA real-time webpage (<http://lightning.nmt.edu/hstnlma/current>), while archived real-time quality data by points and density can be viewed in ten-minute and hourly increments at <http://lightning.nmt.edu/hstnlma/>.

### **3.4 Data Processing**

While the decimated data is suitable for real-time applications of the Houston LMA data, it is preferred to use the full, undecimated dataset for research purposes. As mentioned in the previous section, the LMA system detects VHF sources with a time resolution of 80 microseconds. Due to bandwidth limitations, the undecimated data cannot be transmitted in real-time back to a central LMA server. Therefore, an 80 GB solid state data drive is included within the LMA enclosure of each sensor. Data are written to this drive throughout the day. Each day, data from the previous day are transmitted over the cellular data network back to a central LMA server using an rsync process. It takes approximately two hours to send a day of data from one station. To reduce the potential for diminished performance of the real-time data stream, the stations begin sending their data at staggered times during the day. With 12 stations in the network, it is unlikely that previous day's data will be transferred from more than one site at a given time. To prevent data loss in the event of a temporary loss of network connectivity, the data hard drive disk will continue to store the raw data. If the data drive fills up, it will begin overwriting the oldest data first, so the most recent days will be preserved. Using the rsync process, previous data will be backfilled once the cellular

data network connection is restored. Alternatively, if circumstances dictate, data can be manually retrieved from the field station data hard drive disk during a visit to the sensor site.

After the raw, undecimated data from each station are transferred back to a central LMA server, these data will be processed using the `lma_analysis` program developed at New Mexico Institute of Mining and Technology. A location file has been generated for the network containing the three-dimensional position of each of the sensor locations. Utilizing the precise time of arrival of the LMA source at multiple sensor locations, the location and time of a VHF source can be calculated. While only four sensors are required to solve the system of equations to locate the VHF pulse in time and space, it is desirable to reduce the potential error in locating the pulse. The inclusion of additional sensors serves to reduce location errors. For the processing of data for the Houston LMA network, an LMA source must be detected by no fewer than six sensors to be accepted as a valid solution. Following the processing, the solutions of valid LMA sources are written to a file with parameters including time (to nanosecond resolution), latitude and longitude (to eight decimal places), altitude, and maximum power. These files are moved to permanent storage and held for analysis. A script was created to facilitate automated processing of a full day of data. The script processes data after a seven-day delay to give enough time for the raw data to be copied to a central server, even in the event of temporary loss of cellular data connectivity or other issues. If any missing data are recovered after the initial processing, the analysis code should be run manually with the new data to improve the accuracy of the LMA source solutions.

## 4. DATA AND METHODOLOGY

### 4.1 Houston Lightning Mapping Array

The Houston LMA data received from each sensor site are processed on a central LMA server, as described in the previous section about network operation. As a total lightning detection network, the LMA detects VHF sources in both IC flashes and the IC portions of CG flashes. No differentiation is made in the data collection, but some information can be inferred when performing analysis of sources when grouped into individual flashes. The LMA data were initially processed using the LMA Analysis program developed at New Mexico Institute of Mining and Technology using default settings and parameters. The LMA Analysis program receives the raw data from each station and a list of station locations as input and solutions are written out to a new data file. Valid solutions must be detected by no fewer than six stations and have a reduced chi-square value (a measure of goodness of fit and error minimization between the matrix of times-of-arrival at each sensor and the matrix of time-of-arrival solutions) no greater than five. These output files contain station data that were processed in ten-minute intervals, resulting in an output file of LMA source locations generated for each ten-minute period. Each file contains the time (with nanosecond precision), latitude and longitude (in degrees to eight decimal places), altitude, reduced chi-square value, received power, and a station mask that indicates which stations contributed to each solution. Archived data from the network are available from July 2012 through the

present. The Houston LMA operated as an 11-station network through August 22, when the twelfth sensor was deployed to its location on the Texas A&M – Galveston campus.

#### **4.2 National Lightning Detection Network**

As mentioned in the background section, the National Lightning Detection Network (NLDN) is a low frequency (LF) network of more than 100 sensors utilizing combined time-of-arrival and magnetic direction finder technology to detect and locate CG lightning strokes in two-dimensions. Vaisala, Inc. manages and operates the NLDN from the Network Control Center, located in Tucson, Arizona. Real-time data from this network are displayed at TAMU on a workstation beside real-time LMA and radar displays, and this facilitates comparison between these datasets on an observational basis while events are in progress. However, this is only a display and NLDN data are not archived as they occur; instead, a compact disc (CD) is sent from Vaisala to TAMU on a monthly basis. This CD contains post-processed NLDN data for the previous calendar month and includes date, time (with nanosecond resolution), latitude, longitude, peak current, and polarity. Using processing algorithms provided by Vaisala, the stroke data can be grouped into flashes by spatial and temporal to derive multiplicity of flashes.

#### **4.3 Network Range and Accuracy**

Before performing any analysis involving the Houston LMA data, it is important to establish the effective range of the network for operational purposes. Additionally, a sense of the accuracy of the network in mapping LMA sources in three-dimensions serves as a fundamental foundation for any research use of data from the LMA. Geometric models have been developed at New Mexico Institute of Mining and



Technology for estimating the uncertainty of located VHF sources, both within and outside of the LMA network (Thomas et al., 2004). Both sounding balloons equipped with a GPS receiver and VHF transmitter and aircraft based measurements validated these geometric models for location uncertainty of VHF sources. This method divides analysis of location uncertainty into two sections: sources within the network, and sources outside of the network. The following subsections detail the Thomas et al. (2004) geometry as it will be applied to evaluating the Houston LMA network. For full derivations and additional discussion, the reader should consult this publication.

#### *4.3.1 Location Uncertainty Within the Network*

The geometry of locating VHF sources over the network (that is, within the locations bounded by an oval encompassing the twelve sensor sites) involves the mapping of the plan (two-dimensional) location and the altitude. Sensors located across the network and further from the source are mostly responsible for narrowing the horizontal source location. As illustrated in Figure 9, the uncertainty from stations in different directions produces a circle of diameter  $2\Delta d$  enclosing the source, where  $\Delta d$  is the location uncertainty. Therefore the uncertainty  $\Delta d$  is solved by:

$$\Delta d = c * \Delta t \quad (4.1)$$

where  $\Delta t$  is the root mean square (rms) value of timing uncertainty.

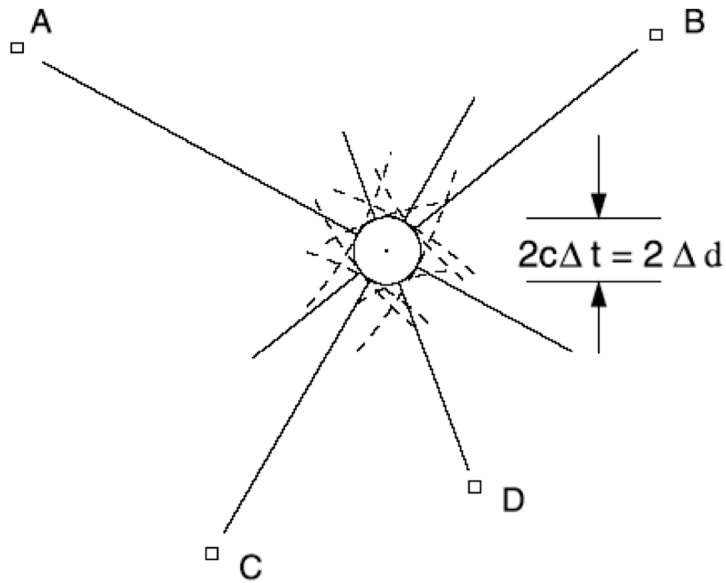


**Figure 9.** Schematic representation of the geometry for locating the horizontal location of an LMA source within the network. Adapted from Thomas et al. (2004).

While distant sensors are responsible for narrowing the horizontal location of an LMA source, it is the closest sensor to the source that is responsible for reducing the altitude uncertainty. As modeled in Figure 10, we can define the location of the source in terms of  $r$ , the radial distance from the nearest station, and  $\theta$ , the elevation angle of the source from the nearest station. We note that the uncertainty is minimized for a source directly overhead, while the error increases as  $r$  increases. From solving the geometry of the figure, we are left with the resulting error parallelogram and can calculate the vertical uncertainty of the LMA source by:

$$\Delta z = c * \Delta t * ((d + r)/z) \quad (4.2)$$

As previously mentioned, Thomas et al. (2004) validated these geometric models and equations by utilizing balloon soundings with an attached VHF transmitter. Furthermore, the results from this geometry were found to be consistent with both the hyperbolic models developed by Proctor (1971) and with error estimates from the linearized forms of the solution equations (Thomas et al., 2004). The resulting location estimates largely agreed between this simpler geometric method and these other techniques.

#### *4.3.2 Location Uncertainty Outside of the Network*

The geometric model for location accuracy of LMA sources outside of the network is based upon a five sensor LMA network arranged along two perpendicular baselines (as illustrated in Figure 11a). Networks with additional sensors, as in the Houston LMA network, contain additional redundancy but are deployed over a somewhat circular arrangement. This ensures there will usually be stations located both parallel and perpendicular to the direction of the source. Furthermore, the geometric model utilizes the sensor closest to the source outside of the network boundary; by definition, this means these results are most typically dependent on the diameter of the network, as these are the distances of the farthest sensors from the center location. The locations of a source can be described in spherical coordinates from the center of the network, given the range, azimuth, and elevation ( $r, \theta, \phi$ ).

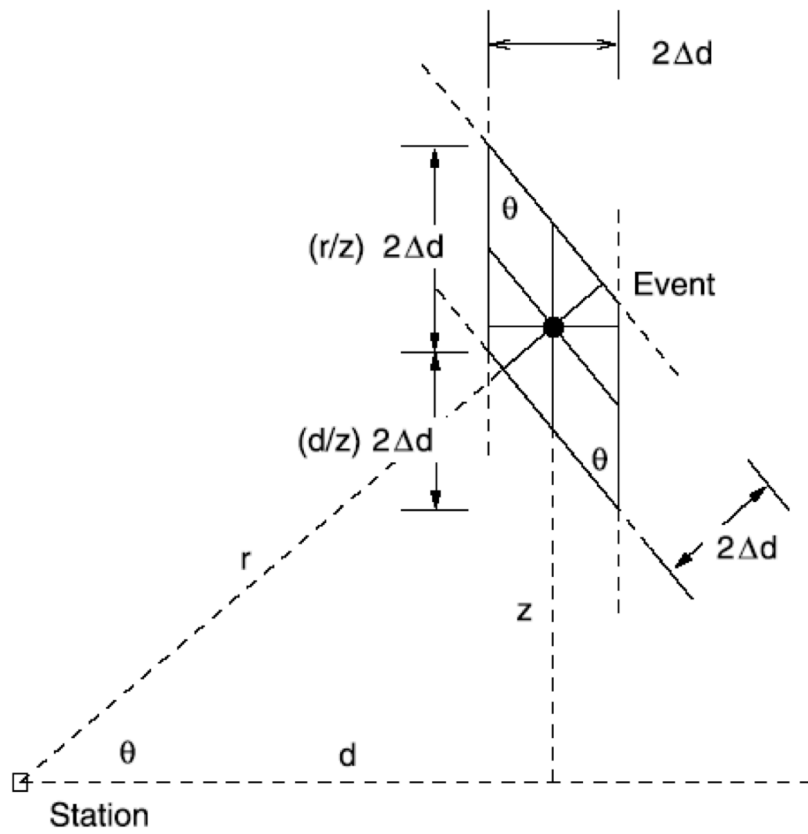


**Figure 10.** Schematic representation of the geometry for determining location uncertainty in the altitude of an LMA source within the network from the nearest LMA sensor. Adapted from Thomas et al. (2004)

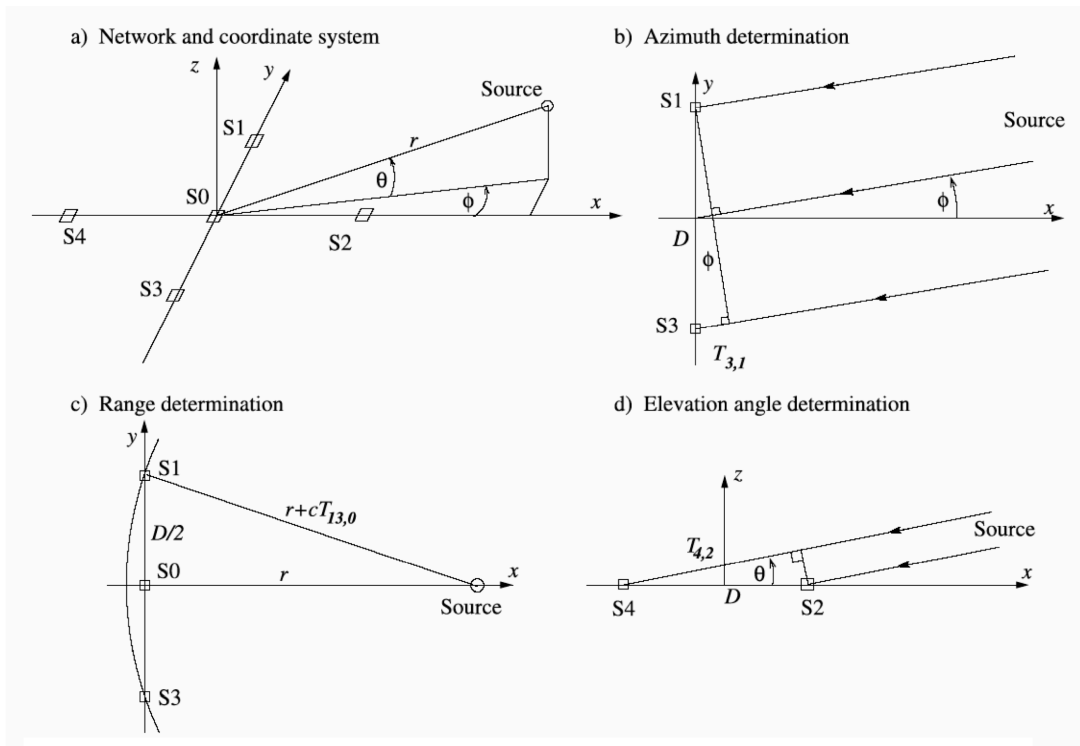


**Figure 11.** Schematic representation of the basic geometry for locating an LMA source outside of the boundary of LMA sensors. The panels illustrate a) the arrangement and coordinate geometry of a conceptual five station LMA network, and the geometric model used to calculate b) the azimuthal angle,  $\phi$ , c) the horizontal range,  $r$ , and d) the elevation angle,  $\theta$  for a source located to the right of the network beyond the network's outer boundary. Adapted from Thomas et al. (2004).

The azimuth position and error estimation is determined by the length of the baseline perpendicular to the direction of the source. Utilizing the first-order approximation that the wavefront is planar, the time-of-arrival difference between the two perpendicular stations (here, T1 and T3 in Figure 11b) enables the calculation of the azimuth angle,  $\phi$ . Further assuming that this angle is small, the geometry can be solved to demonstrate that the position uncertainty in the  $y$  direction is:

$$\Delta y = r\Delta\phi = (r/d) * c \Delta T_{3,1} \quad (4.3)$$

where  $\Delta T_{3,1}$  is the timing difference between stations S1 and S3.

Next, the range of the LMA source can be estimated using the geometry established in Figure 11c. In this example, the error in x position is set to be zero as, to a first order, the source lies along the x-axis. Additionally assuming that S1 and S3 are the same distance from S0, the source reaches both S1 and S3 at the same time (that is, the timing error is the same from S0 to S1 and S0 to S3). Therefore, defining  $\Delta T_{13,0}$  as the difference in time of arrival at S1 (or S3) and S0 results in a measure of the curvature of the waveform of the LMA source, which can be used to solve for the slant range. Thus, the root mean square uncertainty for slant range is:

$$\Delta r \cong 8 (r / D)^2 * c \Delta T_{13,0} \quad (4.4)$$

Finally, we consider the vertical location accuracy of a VHF source detected by an LMA network. While the previous calculations for locating sources beyond the boundary of the network sensors utilized the perpendicular baseline, the parallel baseline (sensors S2 and S4 in this example) is used to estimate the elevation angle and vertical uncertainty. From Figure 11d, we observe that for a source located some distance from the network center, the elevation angle is usually small, which results in very little time-of-arrival difference between stations S2 and S4. Therefore, small timing errors generate large elevation angle errors. Applying trigonometric identifies, the uncertainty in elevation angle can be given by:

$$\Delta\theta = (c * \Delta T_{4,2}) / (D \sin\theta) \cong (r/D) * (c \Delta T_{4,2} / z) \quad (4.5)$$

where  $z$  is the vertical height of the LMA source. The resulting height uncertainty from the elevation uncertainty is:

$$\Delta z_{\theta} = r \Delta \theta = (r^2 / D) * (c \Delta T_{4,2} / z) \quad (4.6)$$

It is worth noting that some height uncertainty is introduced by the error in locating the range to the source. However, Thomas et al. (2004) notes that this contribution is significantly smaller for networks with a sufficiently large diameter, as in the case of the Houston LMA.

#### 4.3.3 Other Considerations

In the above sections, the root mean square timing error was symbolized by  $\Delta T$ . This is one of three variables in the fundamental equation by which the solutions of accepted LMA sources are resolved; namely, rms distance error is the product of speed and the rms timing error. As part of the solution process, the algorithm seeks to minimize the total errors in the location uncertainties. Through an analysis of the goodness of fit values for the solutions, we can gain additional insight into the timing accuracy of the network. The reduced chi-square value is used as the goodness of fit metric, and is defined as:

$$\chi_v^2 = \chi^2 / df \quad (4.7)$$

where  $df$  is the number of degrees of freedom (number of sensors -4) and  $\chi^2$  is the chi-square value defined as:

$$\chi^2 = \sum_{i=1}^N \left[ (t_i^{obs} - t_i^{fit})^2 / \Delta t_{rms}^2 \right] \quad (4.8)$$

which is the summation of difference between the measure arrival time and the predicted arrival time at the  $i$ th station, divided by the square of the rms uncertainty of the measurements of the time-of-arrival of the source at a station. Comparing the reduced chi-square to the theoretical distribution of errors enables an assessment of the actual timing errors present in the LMA data (Thomas et al., 2004).

As mentioned in section 3.2 of this thesis, detection of VHF sources is limited by line of sight. Care is taken when selecting installation locations to prevent any obstructions to the horizon greater than 1 degree, but some obstructions may nonetheless exist. A geometric argument will be presented for investigating the potential impacts of line-of-sight issues upon the Houston LMA dataset. Curvature of the earth becomes a limiting factor when attempting to detect near-ground sources with increasing distance away from the network. Comparisons of NLDN and LMA data assist in determining the realistic detection efficiency at distances far from the center of the LMA network. Likewise, comparison of LMA and radar data can prove useful, accepting the assumption that constant returns in radar reflectivity should correspond to constant lightning activity.

#### **4.4 Source and Flash Analysis**

After establishing the theoretical and effective range of the Houston LMA network, it is desirable to begin a basic analysis of sources detected by the LMA. As mentioned in section 3.4, network data are processed into ten-minute files and stored for analysis. These post-processed files are viewed using *xlma*, a software package built in IDL by researchers at New Mexico Institute of Mining and Technology. The software,



shown in figure 12, enables the display and analysis of LMA data. Data from the NLDN can be imported, allowing the overlay of LMA total lightning and NLDN CG strike data. Using this software, the distribution and structure of LMA sources can be plotted. Using the inferred charge identification technique, which follows from the bidirectional lightning propagation model (Wiens et al., 2005), it is assumed that flash initiation occurs in regions between strong opposite charges and subsequently propagates in both directions into the charged regions. This breakdown inherently generates higher power at the VHF frequencies detected by LMA, which results in far more detected sources depicting the negative breakdown process. From this assumption, a flash will typically have many more sources mapped within the positive charge region of the cloud (Rison et al., 1999). Watching an animation of sources can be useful to diagnose charge structure, as the initial sources are assumed to be associated with negative breakdown, and these first points of a flash are inferred to move towards positively charged regions and away from negative charge. Thus, most IC flashes demonstrate layers of vertical stratification with far fewer sources, if any, in the inferred negative region than the inferred positive region (Tessendorf et al., 2007).

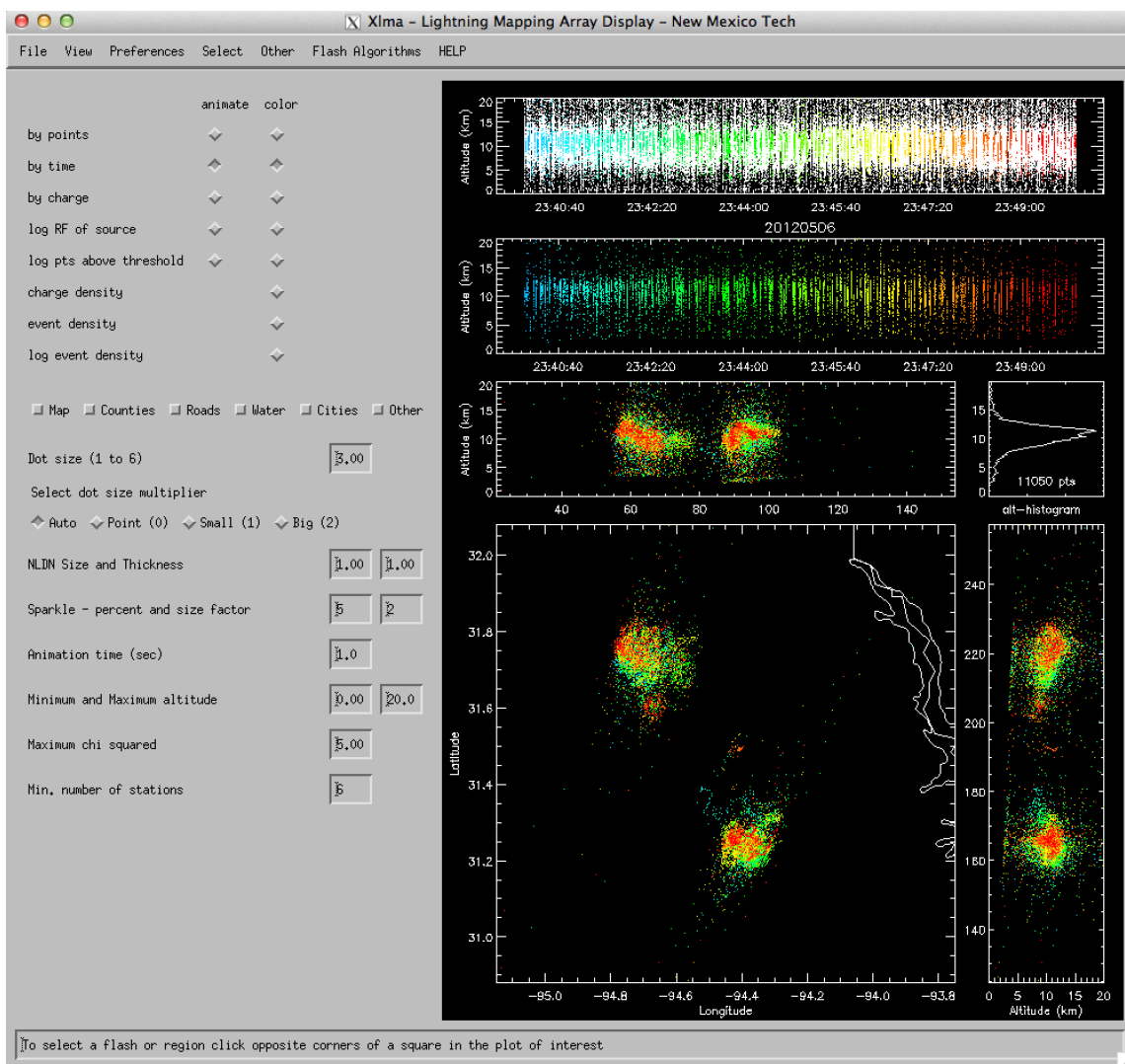


**Figure 12.** Screenshot of the xlma software package displaying ten minutes of Houston LMA data. The left side provides various configuration and display options, while the data is displayed in the six panels on the right side.

## 5. RESULTS

### 5.1 Network Location Accuracy

As previously discussed, the Houston LMA network is a twelve-sensor array with an inner ring of ten sensors circling the Houston metropolitan area and two additional sensors. This was necessary due to the unique challenges of installing an LMA network in the core of a highly developed urban environment. Instead, these two sensors – installed in College Station and Galveston – serve to provide decreased location uncertainty in detecting sources in these regions.. Installing the final two sensors inside the city would have maintained the 80km baselines in both the North-South (N-S) and East-West (E-W) directions while operating with diminished performance due to increased local noise. Instead, the stations at Galveston and College Station, at a distance of 70km and 130km, respectively, from the network center, increase the baselines of the network. This has dual impacts: first, College Station and points southeast now become inside of the array, and second, the increased baselines will enable decreased error for sources outside the array. Figure 13 provides an annotated schematic of the primary baseline lengths and other important distances between sensors in the Houston LMA network. Without a sensor at College Station, we consider the vertical accuracy of a source in this region. This would be governed by equation 4.6 for  $r=130\text{km}$ ,  $D=80\text{km}$ ,  $\Delta T=30\text{ns}$ , and  $z=10\text{km}$ , yielding an uncertainty  $\Delta z$  of approximately 200m. After the inclusion of the sensor at College Station, a source located, for example, 10 km southeast of the sensor site, would now be inside of the array and governed by

equation 4.2. Solving the equation for a source still at 10km, the altitude error is reduced to only 20m. Therefore, the placement of this site to the northwest of the center of the network greatly increases location precision by extending the within-network area beyond just the core of metropolitan Houston. The previously installed LDAR-II network calculated about 1km uncertainty in vertical location for a source at this height, so the installation of the LMA represents a significant improvement in location accuracy for areas to the northwest of Houston (Ely, 2008). Similar improvements are also found for the area between south Houston and Galveston with the addition of a sensor there (Bill Rison, personal communication).

While the most significant detection improvements exist by regions moving from outside to inside of the Houston array, the increased north-south baseline length also improves detection accuracy for points outside of the array. Recall from section 4.3.2 that azimuth and range error are determined by the perpendicular baseline, while altitude error is determined by the parallel baseline. Therefore, for sources located outside of the array, the extended N-S baseline will decrease azimuth and range error for sources located to the east and west of the array. Similarly, sources to the north and south of the network will have a decreased altitude error due to this longer baseline.

As mentioned in section 4.2.3, comparing the reduced chi square metric to a theoretical distribution can assess the timing error of the network. We analyze the case of May 6, 2012, which was the first significant storm after installation of the Houston LMA. While somewhat north of the core of the array, it was certainly within range of the network as it moved through the College Station area. This event was just a few weeks

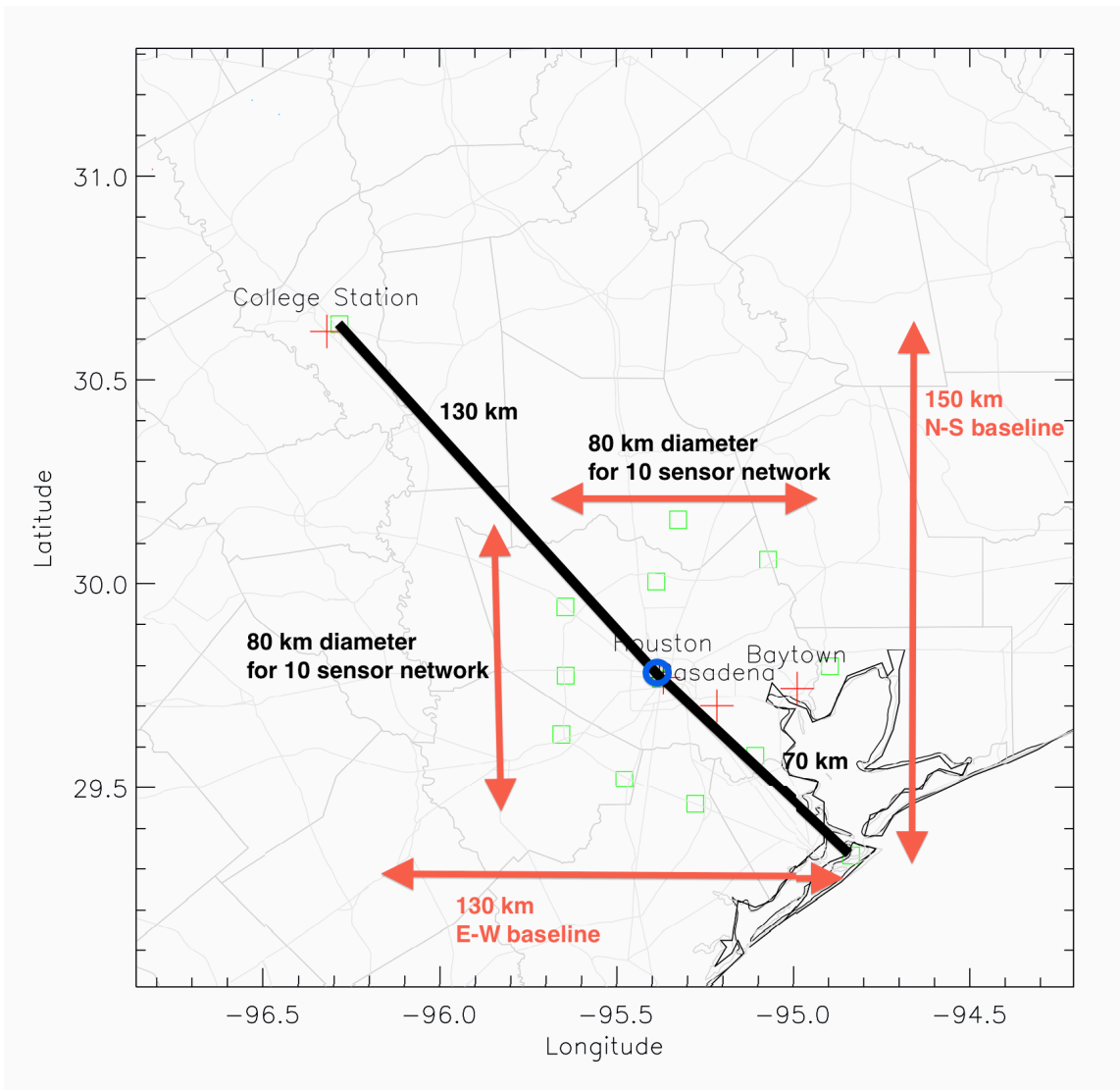


**Figure 13.** Plot of LMA sensors with primary baseline lengths overlaid. Note that the inner ten-station core is roughly circular with 80km baselines in both the North-South and East-West directions. The addition of the two sensors in College Station and Galveston extends the baseline to 150km N-S and 130km E-W. The blue circle indicates the center of the network.

after network installation and eleven stations were participating in solutions. Two stations were installed at the College Station site (one would be moved to Galveston in August 2012), and including both would have greatly increased local noise sources because they would have correlated noise. While the Houston LMA was not as sensitive as other more remote installations, network performance was quite strong. Data were plotted for a half-hour period from 2300 to 2330 UTC on May 6, 2012. Figure 14 shows a plot of  $\chi_v^2$  values from the detected LMA sources versus the theoretical  $\chi^2$  distribution. A different plot is created for solutions containing a particular number of contributing stations, as the number of degrees of freedom is the number of sites participating in a solution minus four. Note that the dots match with the solid line (theoretical distribution) quite well across the range of seven to eleven sensor solutions. This timing error of 25ns is quite good in comparison to the STEPS (43 to 55ns) and Oklahoma LMA (38 to 45 ns) networks (Thomas et al., 2004). It is worth noting multiple factors assisted with this minimal timing error. As illustrated in Figure 15, the storms were very close to the TAMU sensor, which would help reduce the vertical error, without significant electrification occurring throughout the rest of the LMA domain. Additionally, all eleven stations were operational and approximately half of all detected sources were resolved by 9 or greater stations. As more cases are analyzed, greater confidence in the typical timing error of the network will develop. Furthermore, the primary cause of deviation between the observed and best-case errors is that typically not all stations participate in solutions. Thomas et al. (2001) demonstrated that most located sources from natural

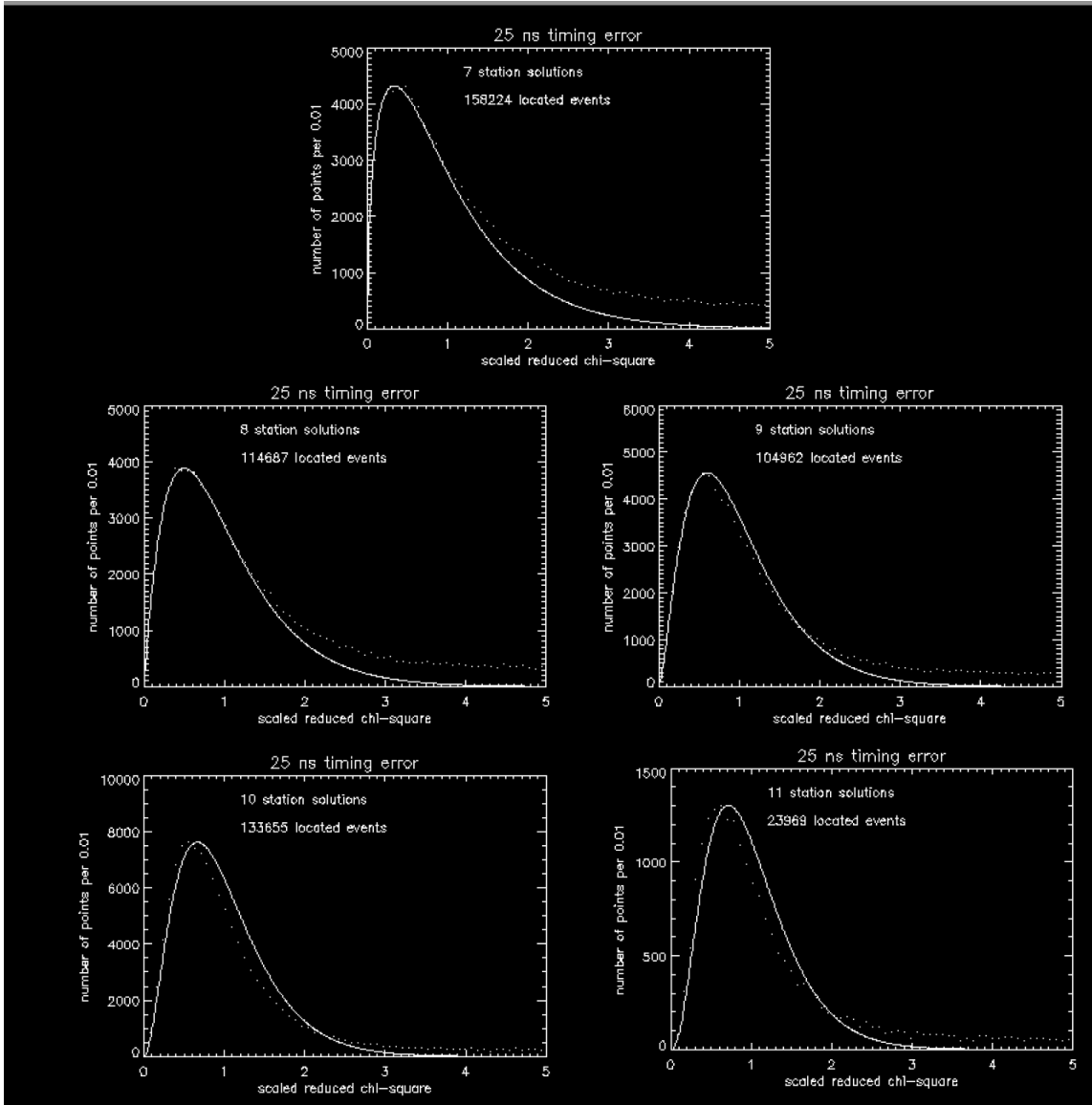


**Figure 14.** Plot of calculated reduced chi-square compared to theoretical chi-square distribution for 25ns timing error for the thirty minute period from 23:00 to 23:30 UTC on May 6, 2012.

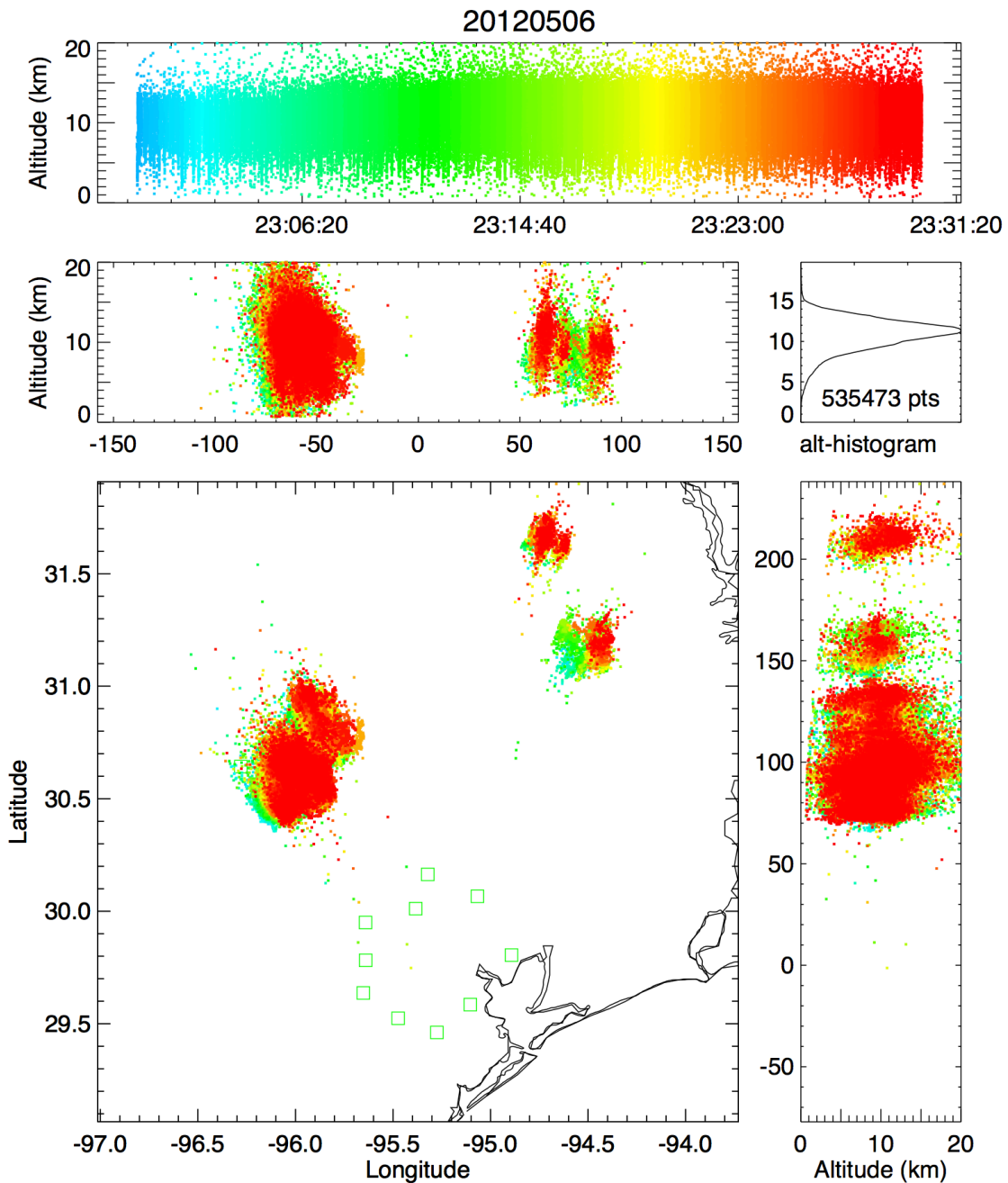


**Figure 15.** Five panel plot of VHF sources from the Houston LMA from 23:00 to 23:30 UTC on May 6, 2012. Note the cluster of activity around the TAMU sensor site, with only two localized storms detected off to the northeast of this area.



lightning are low-power flashes that are resolved by perhaps 6 or 7 sensors. While a larger number of stations make it more likely that events will be detected by a greater number of sensors, Thomas et al. (2004) empirically noted that having more sensors results in the detection of more sources in a given discharge, rather than resulting in a higher number of sensors contributing to each individual solutions.

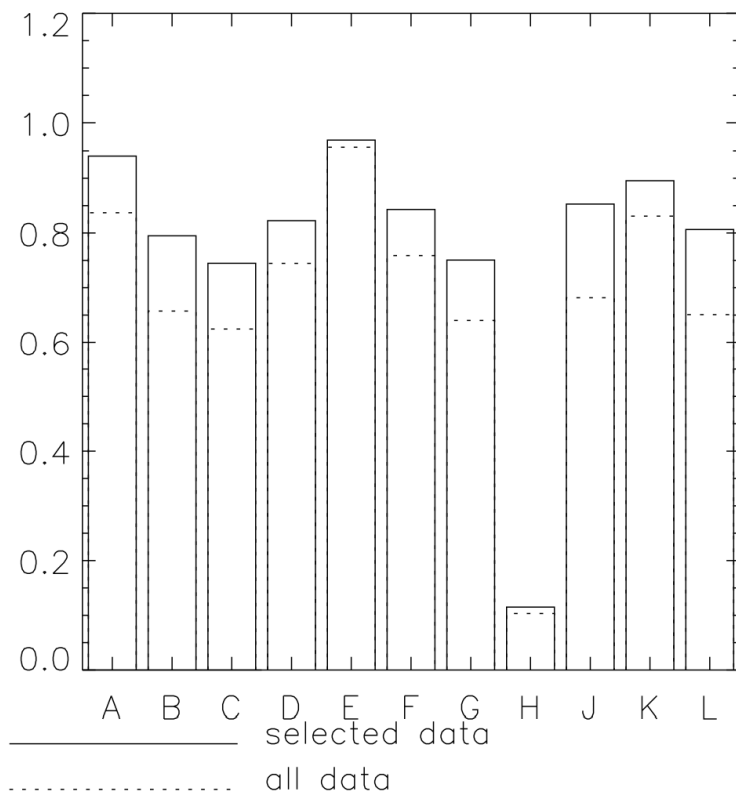


**Figure 16.** Plot of fraction of total sources detected by each sensor for the thirty minute period from 23:00 to 23:30 UTC on May 6, 2012. Station H, located at Houston Raceway, detected fewer than 15 percent of VHF sources.

A look at the fraction of total solutions detected by each sensor is particularly insightful in this case. As shown in Figure 16, ten of the eleven active sensors participated in solutions for at least 75% of total sources. The lone outlier, station H at Houston Raceway on the east side of the network, participated in fewer than 15 percent of the approximately one-half million detected VHF sources during this period.

## **5.2 Network Range and Detection Capability**

As described in section 4.3.3, a few considerations exist when evaluating the detection of VHF sources by the Houston LMA network. In particular, the ability to detect lower level flashes can be obstructed. In line with the LDAR-II installation guidelines, it was attempted to not permit a site to have more than 1 degree of obstruction on the horizon. As illustrated in Figure 17, an obstruction at 1-degree elevation will block sources below 1.7km at a distance of 100km. Empirically, only a small percentage of total sources are detected below 5km from the Houston LMA. Only at significant ranges (about 300km) would this potential blockage start to prevent lower level sources from being detected; however, as will be shown, at this range, detection will drop off for all but the strongest events. Therefore, using the 1-degree elevation angle criteria for installation will preclude significant loss of LMA sources.

Additionally, as sources grow more distant from the LMA network, the curvature of the earth begins to become evident on LMA source plots. The plot in Figure 18 shows one hour of LMA sources from May 12, 2012. Looking at the top plot, a horizontal-vertical cross section, the curvature effect is quite prominently visible past about 100km. At a range of about 250km, this effect prevents sources below 5km from being detected. In

addition to the impact of curvature, some refractive and propagation effects may also contribute to this observation. As such, the analysis of distant points from the center of the network must be carefully considered.

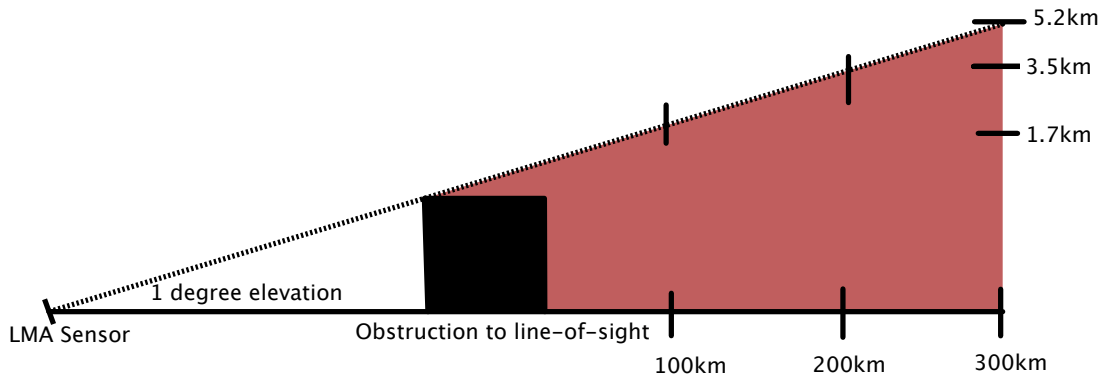


**Figure 17.** Schematic illustration the heights of blockage of VHF sources by a 1-degree elevation angle obstruction at a sensor site. The LMA sensor would not detect any sources in the red shaded area.

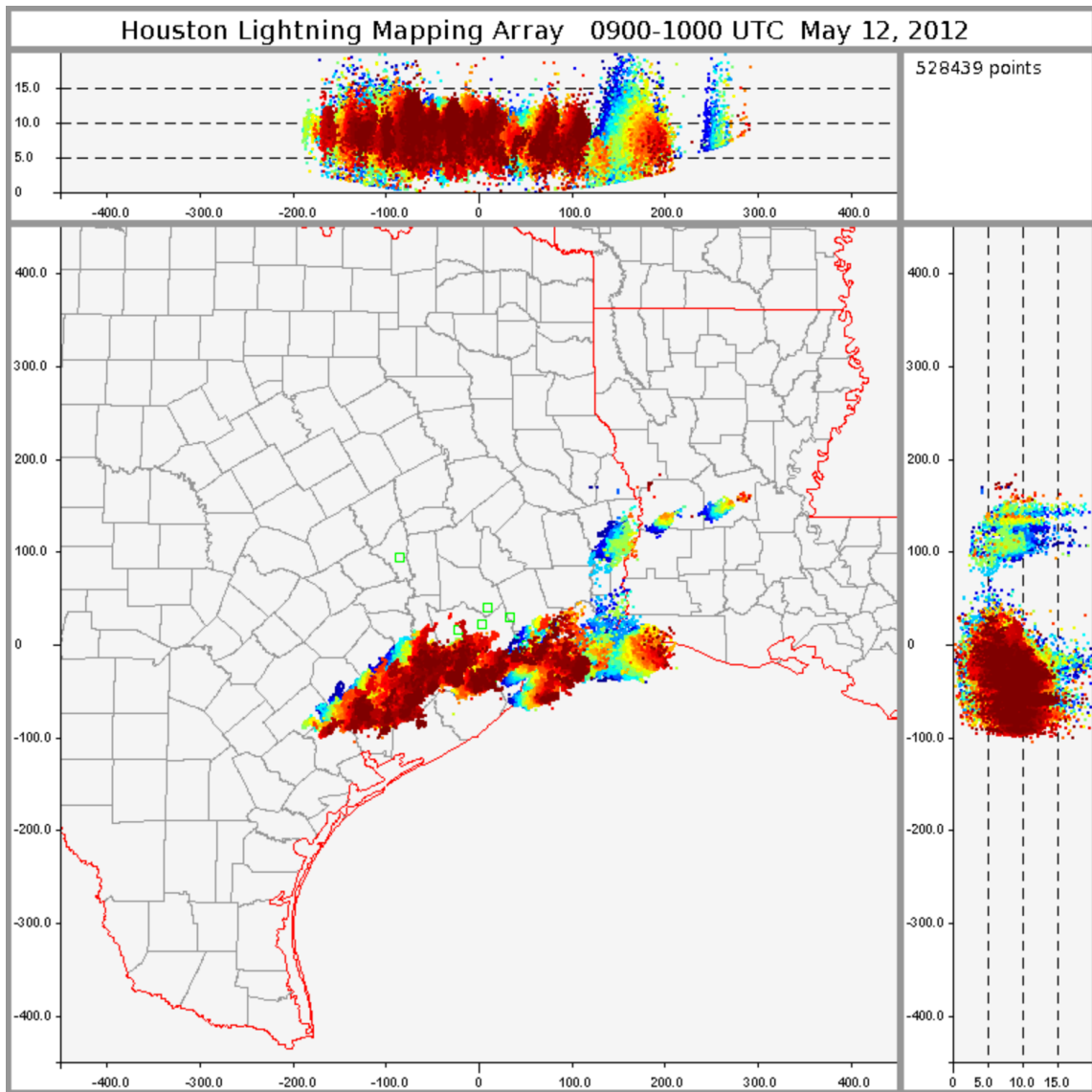


**Figure 18.** One hour plot of LMA sources detected from 09:00 to 10:00 UTC on May 12, 2012 illustrating the impact of the curvature of the earth when detecting sources at a distance from the network center.

Taking into account these inherent limitations, we now move to addressing the effective range of the Houston LMA network. It would be desirable to plot all sources detected by the LMA network as a function of range from the center network and the resulting density of sources to establish a threshold distance beyond which sources drop off. However, at this time, an insufficient amount of data is available to perform this analysis, and this must be held for future work. However, an observational analysis that demonstrates an approximate effective range of the Houston LMA network will follow.

A significant line of the thunderstorms moved through southeast Texas on the morning of May 10, 2013. Looking at 0.5 degree reflectivity scan from the KHGX National Weather Service radar, we see a large squall line stretching through the Houston metropolitan area and stretching east to the Texas/Louisiana state line and southwest toward Corpus Christi. This line pushed consistently towards the southeast over time maintaining a consistent reflectivity signature with a central region of the line maintaining reflectivity measuring 50-60 dBz. Figure 19 shows the reflectivity as it passed through the Houston metropolitan area. Looking at real-time CG data from the NLDN over a thirty-minute period (1545-1615 UTC; 10:45-11:15am local), shown in Figure 20, we note that the rate of ground strikes detected is approximately constant at 1,000 per five minutes, or 200 per minute, over this time. Additionally, the strikes are distributed throughout the entire line where the radar data indicates the maximum reflectivity values. We make the assumption that given the consistent radar and NLDN presentation, the total lightning characteristics should also remain approximately

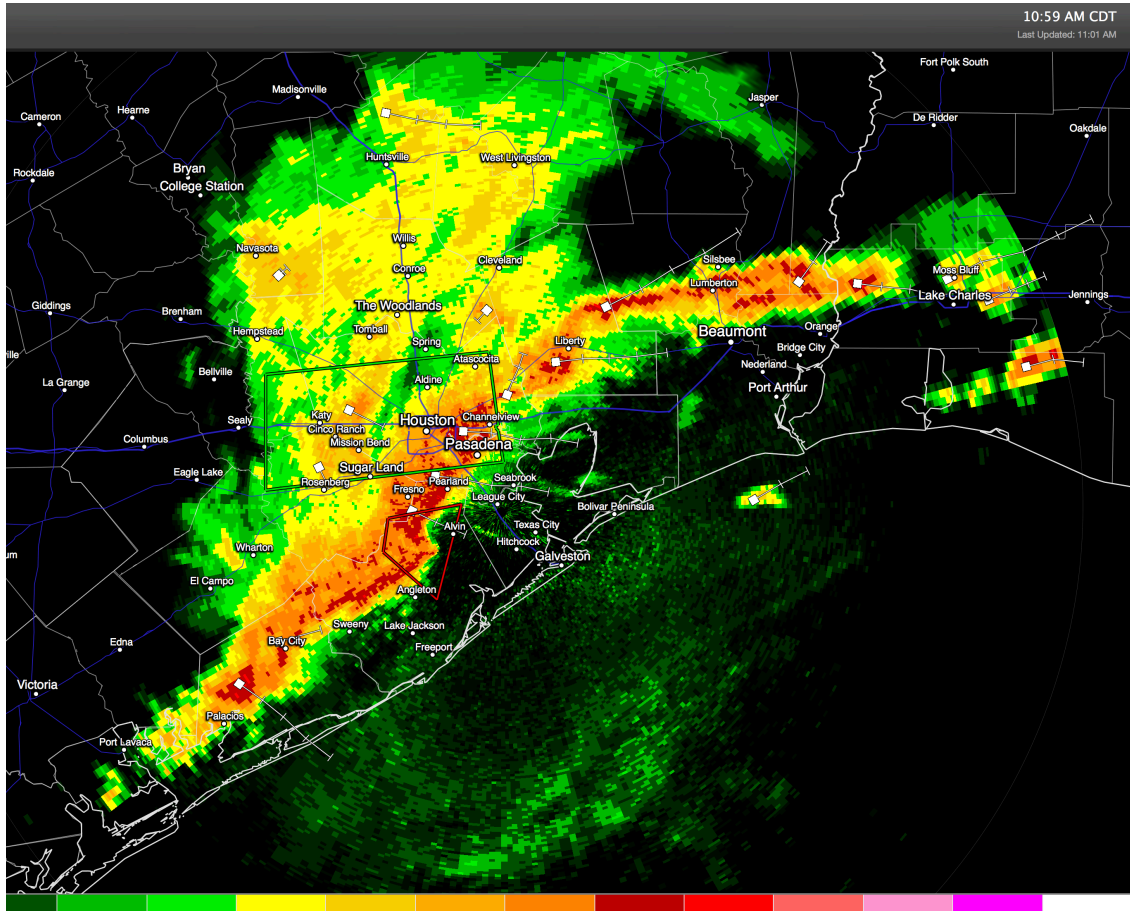


**Figure 19.** Radar reflectivity from KHGX radar at 15:59 UTC on May 10, 2013 showing the line of strong storms pushing southeast through the Houston metropolitan area.

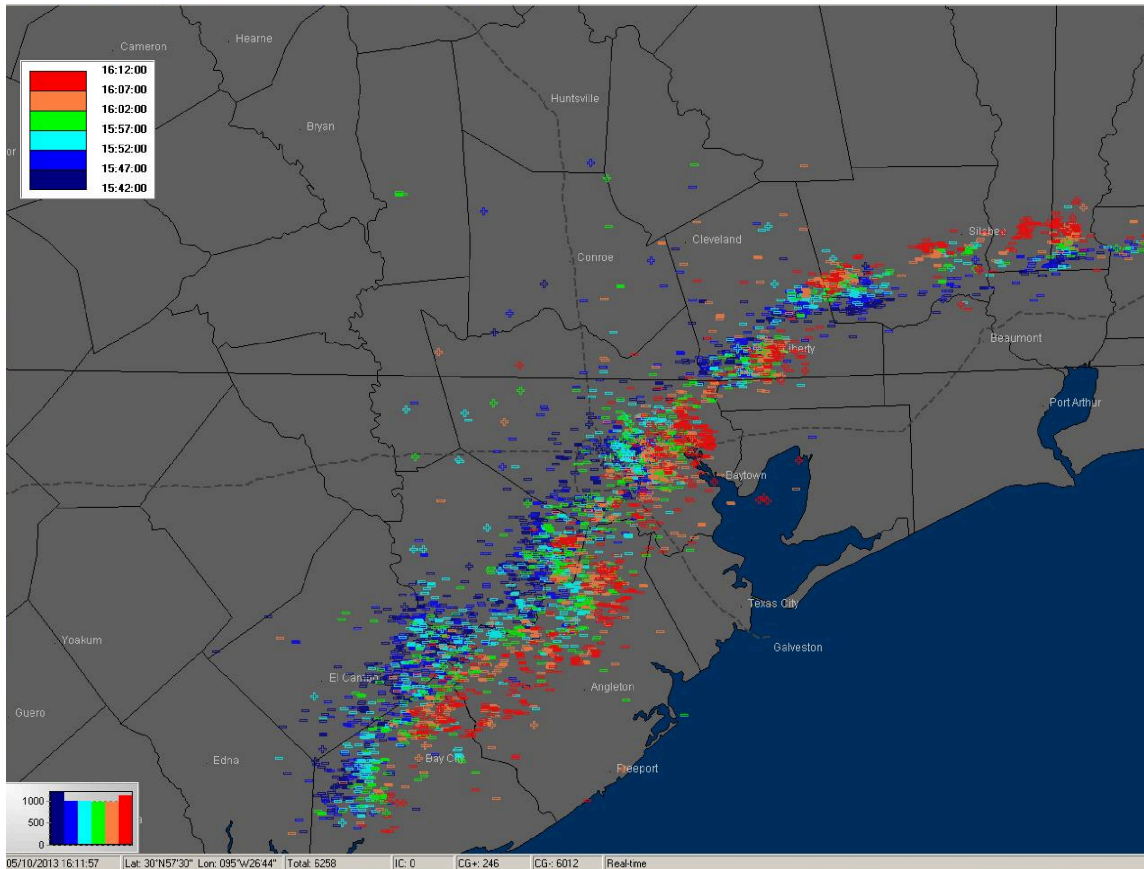


**Figure 20.** Plot of CG strikes from the NLDN from 15:45 to 16:15 UTC on May 10, 2013.

constant. Therefore, this line of storms provides an ideal example to evaluate the range of the Houston LMA network. Ely et al. (2008) utilized a similar technique with the passage of a mesoscale convective system to determine the range of the Houston LDAR-II network.

However, when looking at the Houston LMA data plot, the distance limitations of the LMA network became evident. As evident in Figure 21, VHF sources are detected

with highest numbers in the 10km-15km altitude range out to approximately 100km in both the x and y directions. Basically geometry yields an effective range of just over 140 km in both the northeast and southwest directions. Additionally, low-level sources (~5km) are only detected at close range, out to about 50km, to the center of the network. This lower-level positive charge region is detected for storms over the network center but remains undetected at with increasing radius. Plotting the density of VHF sources rather than the individual points, as shown in Figure 22, further illustrates the diminished detection beyond about 100km in the x and y cross sections, corresponding to a range of about 140km. This is consistent with, but on the lower range of, empirical observations of various storms detected by the Houston LMA. However, this is not entirely unexpected given that only six LMA sensors – the minimum required to resolve a solution – were operational on this day. A second case, from May 6, 2012, illustrates slightly better detection range. On this day, eleven sensors were operating in the Houston LMA network and sources were detected approximately 230km to the northeast of the network center, while only single LMA sources were detected west of Austin (~260km from network center) in association with the NLDN activity as shown in Figure 23. Therefore, we establish the range of the network to be approximately 250km for two-dimensional mapping at full operation. This encompasses both the line-of-sight and curvature considerations previously mentioned.



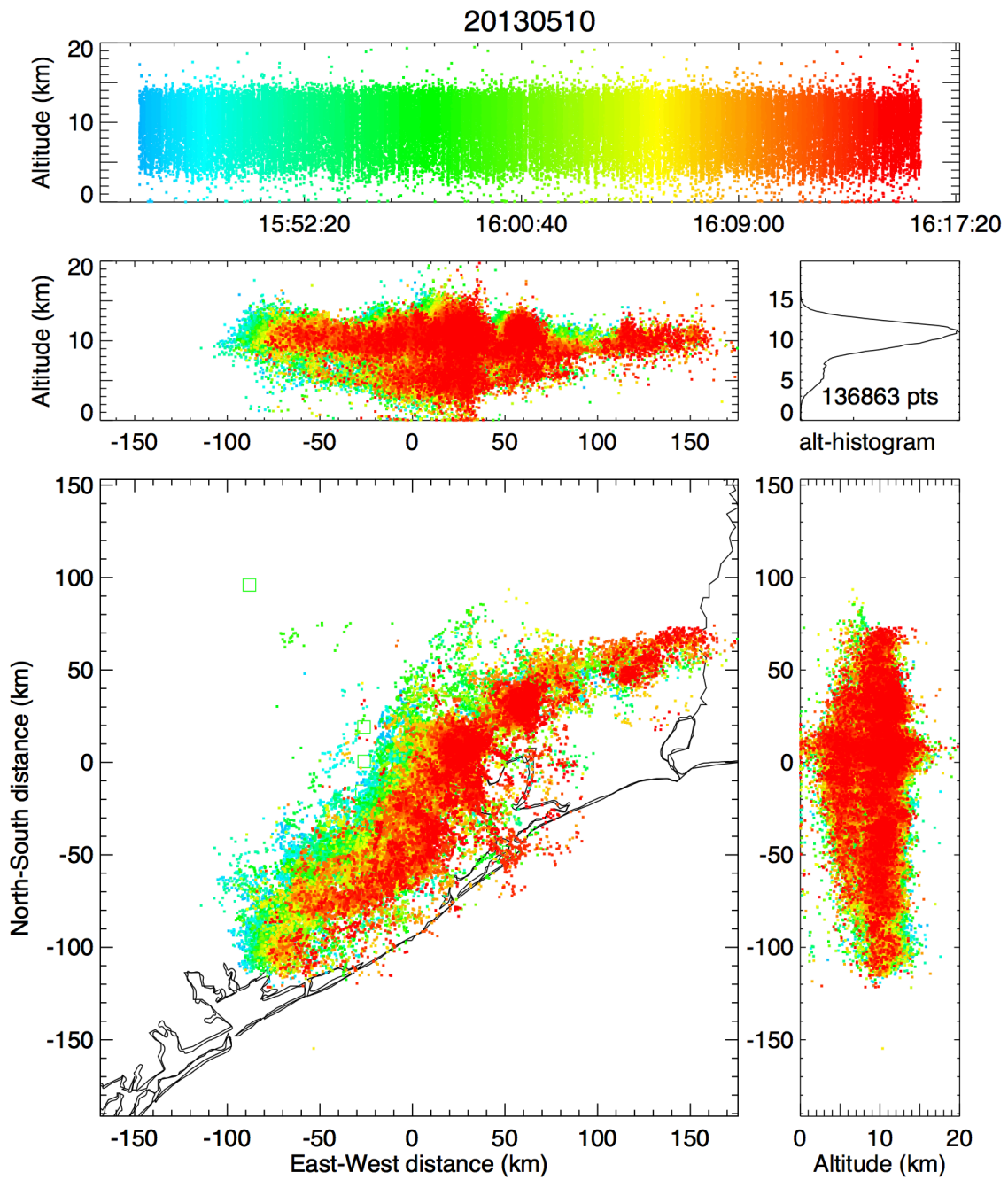


**Figure 21.** LMA point sources from 15:45 to 16:15 UTC on May 10, 2013.

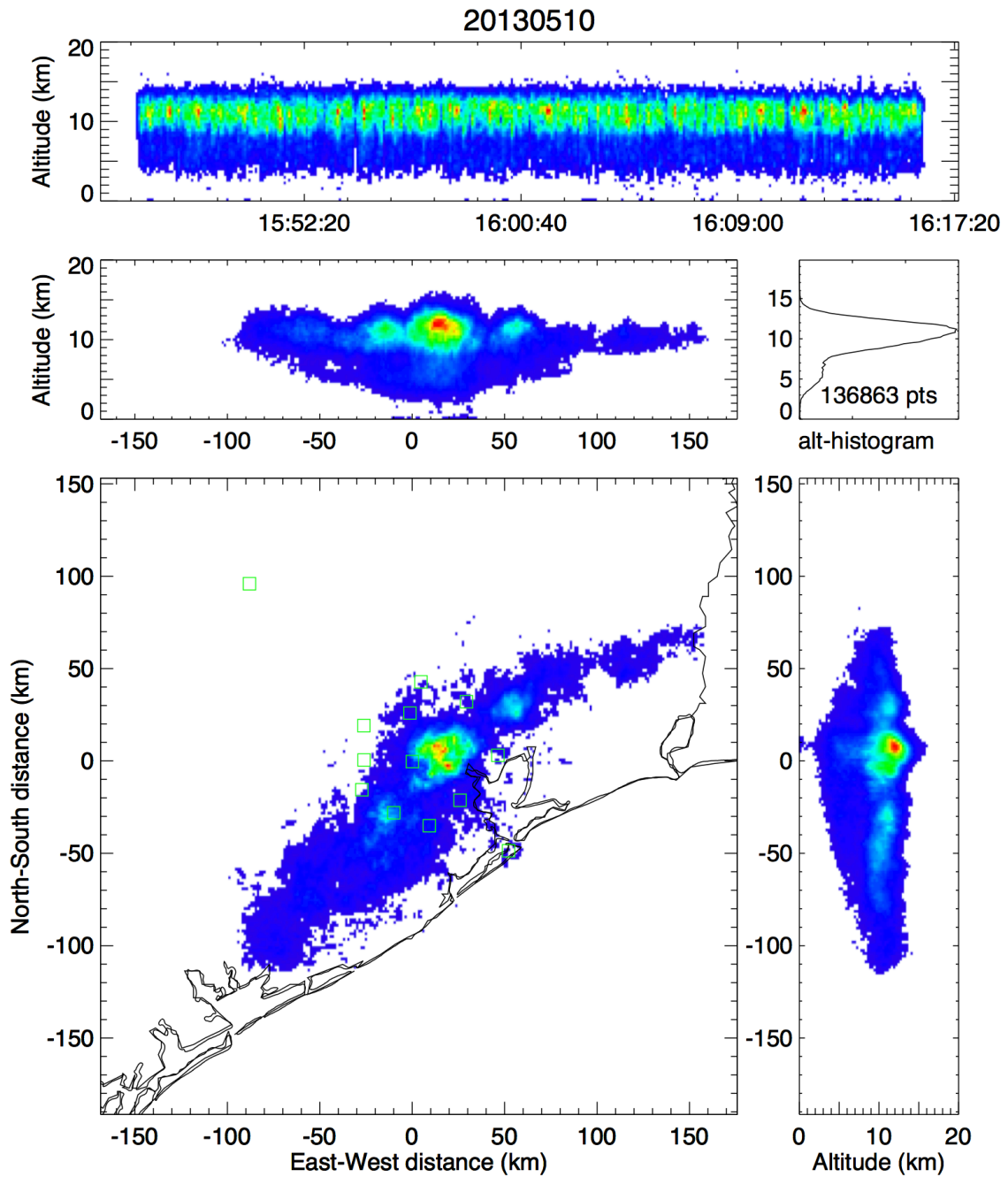


**Figure 22.** Same as Figure 21 but for LMA source density.

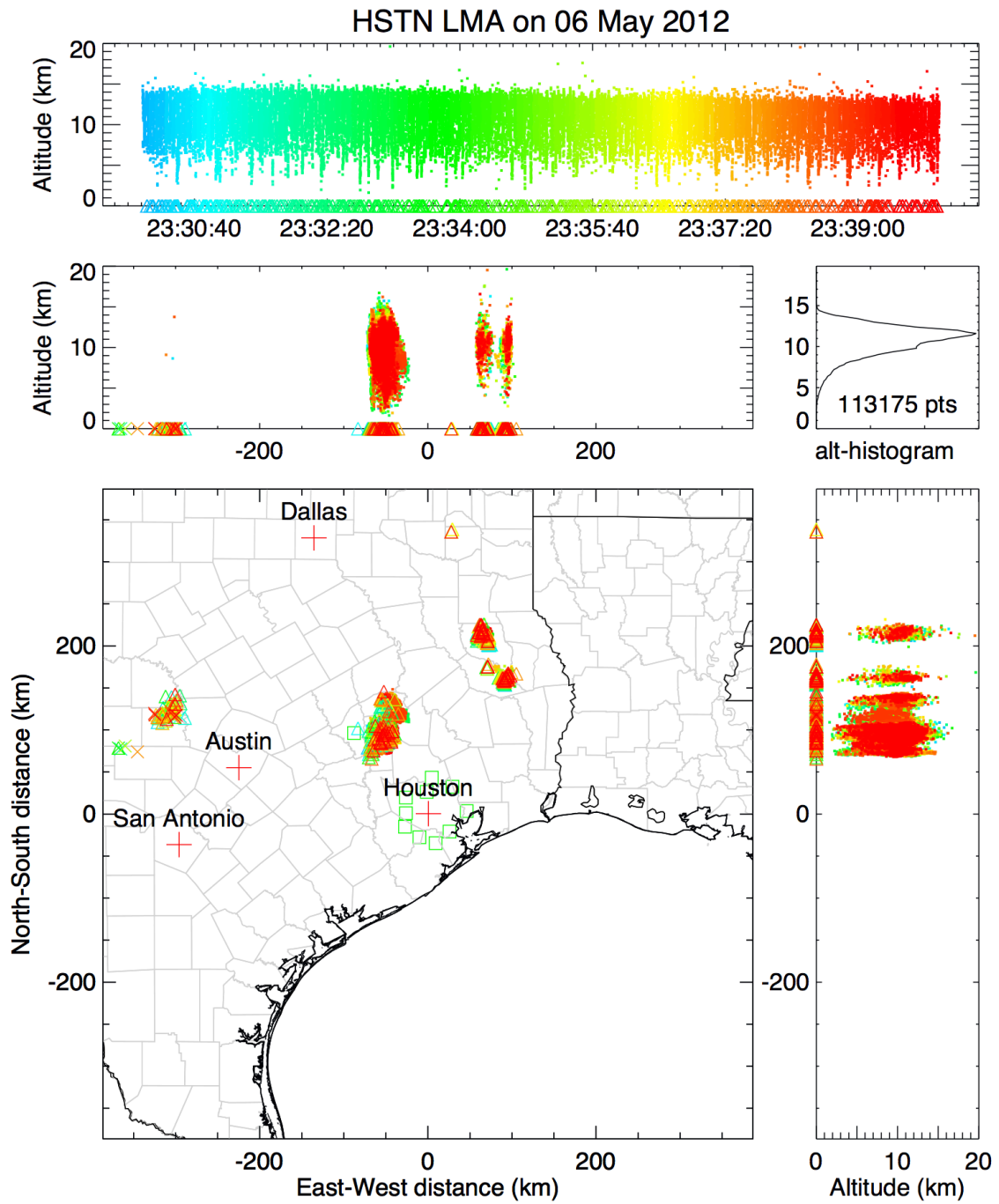


**Figure 23.** LMA sources and NLDN ground strikes detected from 23:30 to 23:40 UTC on May 6, 2012.

### **5.3 Operational Results**

As mentioned during the network operation section, Houston LMA data are transmitted in real-time to partners including the NASA Short-term Prediction Research and Transition Center (SPoRT) and the Houston/Galveston Weather Forecast Office (WFO) of the National Weather Service via the TAMU Department of Atmospheric Sciences' LDM server. These groups utilize data from the Houston LMA network for development, research, and operational uses. While WFO Houston/Galveston has only recently begun receiving the data, forecasters have found great value in utilizing total lightning data for increasing lead-time when issuing amendments to their Terminal Aerodrome Forecasts (TAFs). Furthermore, it is expected that total lightning data will assist forecasters in warning decisions during the summer pulse thunderstorms that are common across the Houston metropolitan area (Lance Wood, personal communication). Additionally, the Houston LMA data are expected to be incorporated into the Hazardous Weather Testbed experiments and the National Lightning Jump Field Test. Therefore, the Houston LMA network is expected to continue to assist operations and development of forecast tools, in addition to serving its primary purpose as a research network.

## 6. CONCLUSIONS

### 6.1 Conclusions

The Houston Lightning Mapping Array is a three-dimensional system that detects VHF impulses that are emitted during the electrical breakdown and lightning propagation process. The network, comprised of ten sensors surrounding the Houston metropolitan area with two additional sensors in Galveston and College Station, provides continuous mapping of total lightning above the network and extending beyond the perimeter of the sensors. The establishment of a total lightning mapping system in Houston is particularly beneficial for multiple reasons. The region experiences cold fronts, sea breeze effects, MCSs, and tropical cyclones and climatologically experiences lightning during all twelve months of the year. The significant population and industry of Houston enables research into the influences of an urban environment on thunderstorm structure and lightning occurrence.

The LMA sensors are built by New Mexico Institute of Mining and Technology and provide an independent, portable design that utilizes solar panels and cellular data modems for power and communications. The LMA network was installed in April 2012, with real-time operation commencing with eleven sensors by the end of the same month. The network was completed in its current form with the deployment of the twelfth sensor to Galveston in late August 2012. The sensors operate in a real-time mode transmitting decimated data to a central server that compiles and processes these data to generate real-time images of lightning activity. These data are distributed in real-time via

a departmental LDM server with the NWS for operational utilization. Additionally, the sensors write the raw, undecimated data to a hard drive and transmit this full dataset each day back to the central LMA server for post-processing, analysis, and archival.

The Houston LMA has a diameter of 150 km from north to south and provides outstanding accuracy from College Station to Galveston, including the Houston metropolitan area. The three-dimensional range of the network extends about 75 km from the network center in downtown Houston, while two-dimensional mapping extends approximately 250 km. These figures are derived from empirical operation and preliminary analysis of the limited dataset available in conjunction with NLDN and radar data. In addition to being maintained as a research network, network data are utilized by National Weather Service forecasters at WFO Houston/Galveston to improve forecast products and serve as a decision support tool for the issuance of warnings.

## **6.2 Future Work**

Now that the network has been established, much work remains to begin developing detailed analyses of thunderstorms occurring over the Houston area. As the temporal coverage of the Houston LMA dataset increases, a climatology of total lightning over southeast Texas can be developed. This, in conjunction with NLDN CG data, will enable a more complete validation of network range to be undertaken. Additionally, the use of LMA total lightning as a predictor of CG activity will be studied. Also, the network data will be utilized to analyze individual flashes to gain insight into key differences in electrification structure, organization, and IC/CG flash rates as compared to storms in other regions of the United States. Finally, the recent

upgrade of the KHGX radar to dual-polarization technology will facilitate comparison of radar and electrification structures within storm cells.

## REFERENCES

- Curran, E. B., R. L. Holle, R. E. Lopez, 2000: Lightning casualties and damages in the United States from 1959 to 1994. *J. Climate*, **13**, 3448-3464.
- Ely, B. L., 2008: Houston LDAR II network: design, operation, and performance analysis. Ph.D. dissertation, Texas A&M University.
- Ely, B. L., R. E. Orville, L. D. Carey, and C. L. Hodapp, 2008: Evolution of the total lightning structure in a leading-line, trailing-stratiform mesoscale convective system over Houston, Texas. *J. Geophys. Res.*, **113**, D08114, doi:10.1029/2007JD008445.
- Goodman, S. J., T. Blakeslee, H. Christian, W. Koshak, J. Bailey, J. Hall, E. McCaul, D. Buechler, C. Darden, J. Burks, T. Bradshaw, P. Gatlin, 2005: The North Alabama Lightning Mapping Array: recent severe storm observations and future prospects. *Atmos. Res.*, **76**, 423-437, doi:10.1016/j.atmosres.2004.11.035.
- Huff, F.A., and S.A. Changnon, Jr., 1973: Precipitation modification by major urban areas. *Bull. Amer. Meteor. Soc.*, **54**, 1220-1232.
- Krehbiel, P. R., R. J. Thomas, W. Rison, T. Hamlin, J. Harlin, and M. Davis, 2000: Lightning mapping observations in central Oklahoma, *Eos Trans. AGU*, **81**, 21-25.
- Krider, E. P., R. C. Noggle, A. E. Pifer, and D. L. Vance, 1980: Lightning detection finding systems for forest fire detection. *Bull. Amer. Meteor. Soc.*, **61**, 980-986.
- Lhermitte, R., and P. R. Krehbiel, 1979: Doppler radar and radio observations of thunderstorms, *IEEE Trans. Geosci. Electron.*, *GE-17*, 162-171.
- MacGorman, D. R., I. R. Apostolakopoulos, N. R. Lund, N. W. S. Demetriades, M. J. Murphy, and P. R. Krehbiel, 2011: The timing of cloud-to-ground lightning relative to total lightning activity. *Mon. Wea. Rev.*, **139**, 3871-3886.
- MacGorman, D. R., W. D. Rust, P. Krehbiel, E. Bruning, and K. Wiens, 2005: The electrical structure of two supercell storms during STEPS. *Mon. Wea. Rev.*, **133**, 2583-2607.
- MacGorman, D. R., W. D. Rust, T. J. Schuur, M. I. Biggerstaff, J. M. Straka, C. L. Ziegler, E. R. Mansell, E. C. Bruning, K. M. Kuhlman, N. R. Lund, N. S. Biermann, C. Payne, L. D. Carey, P. R. Krehbiel, W. Rison, K. B. Eack, W. H.



- Beasley, 2008: TELEX: The Thunderstorm Electrification and Lightning Experiment, *Bull. Am. Met. Soc.*, **89**, 997-1013, doi:10.1175/2007BAMS2352.1.
- Maier, L., C. Lennon, and T. Britt, 1995: Lightning detection and ranging (LDAR) system performance analysis, *Proceedings of 6th Conference on Aviation Weather Systems*, P8.9.
- Orville, Richard E., 2008: Development of the National Lightning Detection Network. *Bull. Amer. Meteor. Soc.*, **89**, 180–190, doi: <http://dx.doi.org/10.1175/BAMS-89-2-180>
- Orville, R. E., G. Huffines, J. Nielsen-Gammon, R. Zhang, B. Ely, S. Steiger, S. Phillips, S. Allen, W. Read, 2001: Enhancement of cloud-to-ground lightning over Houston, Texas, *Geophys. Res. Lett.*, **28**, 2597-2600, doi:10.1029/2001GL012990.
- Poehler, H. A., and C. L. Lennon, 1979: Lightning detection and ranging system (LDAR): System description and performance objectives, *NASA Tech. Memorandum, TM-74105*, 86 pp.
- Proctor, D. E., 1971: A hyperbolic system for obtaining VHF radio pictures of lightning, *J. Geophys. Res.*, **76**, 1478-1489.
- Rosenfeld, D., and M. I. Lensky, 1998: Space-borne based insights into precipitation formation processes in continental and maritime convective clouds, *Bull. Amer. Meteor. Soc.*, **79**, 2457– 2476.
- Rison, W., R. J. Thomas, P. R. Krehbiel, T. Hamlin, and J. Harlin, 1999: A GPS-based three-dimensional lightning mapping system: initial observations in central New Mexico, *Geophys. Res. Lett.*, **26**, 3573-3576.
- Shepherd, J. M., and S. J. Burian, 2003: Detection of urban-induced rainfall anomalies in a major coastal city, *Earth Interactions*, **7**, 1-17.
- Shepherd J. M., H. F. Pierce, and A. J. Negri, 2002: Rainfall modification by major urban areas: observations from spaceborne radar on the TRMM satellite. *J. Appl. Meteor.*, **41**, 689-701.
- Steiger, S., R. E. Orville and G. Huffines, 2002: Cloud-to-ground lightning characteristics over Houston, Texas: 1989-2000. *J. Geophys. Res.*, **107**, D11, 10.1029/2001JD001142.

- Tessendorf, S. A., Rutledge, S. A., Wiens, K. C., 2007: Radar and lightning observations of normal and inverted polarity multicellular storms from STEPS, *Mon. Wea. Rev.* **135**, 3682-3706.
- Thomas, R. J., P. R. Krehbiel, W. Rison, T. Hamlin, J. Harlin, and D. Shown, 2001: Observations of VHF source powers radiated by lightning, *Geophys. Res. Lett.*, **28**, 143–146.
- Thomas, R. J., P. R. Krehbiel, W. Rison, S. J. Hunyady, W. P. Winn, T. Hamlin, and J. Harlin, 2004: Accuracy of the Lightning Mapping Array, *J. Geophys. Res.*, **109**, D14207, doi:10.1029/2004JD004549
- Warner, T. A., J. H. Heldson, Jr., and A. G. Detwiler, 2003: Aircraft observations of a lightning channel in STEPS, *Geophys. Res. Lett.* **30** (19), 1984, doi:10.1029/2003GL017334.
- Westcott, N. E. 1995: Summertime cloud-to-ground lightning activity around major midwestern urban areas. *J. Appl. Meteor.*, **34**, 1633–1642.
- Wiens, K. C., S. A. Rutledge, and S. A. Tessendorf, 2005: The 29 June 2000 supercell observed during STEPS. Part II: lightning and charge structure, *J. Atmos. Sci.*, **62** (12), 4151-4177.